Semi-active vibration control by means of electro-magnetic elements

Darula, Radoslav

Publication date:
2014

Document Version
Publisher's PDF, also known as Version of record

Report no.: 103

Semi-active vibration control by means of electro-magnetic elements

PhD Thesis

Radoslav Darula

Department of Mechanical and
Manufacturing Engineering
Aalborg University
Fibigerstraede 16
DK-9220 Aalborg East
Denmark

The thesis has been written in LaTeX, modifying an unofficial AAU template provided at `http://kom.aau.dk/~jkn/latex/latex.php#phdtemplate`.

Printed in Aalborg, June 2014

ISBN 87-91200-69-5

Abstract

The PhD project is focused on an implementation of the electromagnetic elements, i.e. devices capable to introduce non-linear electromagnetic forces into a mechanical system. Furthermore, as the electromagnetic elements are connected to the electric circuit, serving as a source of electromagnetic force, coupling of three physical domains, namely electrical, mechanical and magnetic, is established. Since the electromagnetic force is of a non-linear nature, the system constitutes a coupled multidisciplinary non-linear problem. In the thesis the non-linear problem is addressed from the analytical view point and a dynamical response at close to resonance operation region is analysed using the method of multiple scales. For the multi degree of freedom system a modal interaction is investigated. The operation regions are identified and discussion on control presented. The parameters of the controller are searched experimentally and the operation regions are verified by means of a numerical experiment as well as using simple experimental set-ups. A rapid reduction of an amplitude of vibration (due to additional damping) as well as natural frequency reduction (detuning of resonance) are identified analytically, as well as experimentally.

Resumé

I dette ph.d.-projekt fokuserer vi på implementeringen af elektromagnetiske elementer i vibration kontrol. Disse elementer introducerer ulineære elektromagnetiske kræfter til et mekanisk system, og de er forbundet med et elektrisk kredsløb. Således sammenkobles disse elementer af tre fysiske domæner: det elektriske, det mekaniske og det magnetiske. Den elektromagnetiske kraft har en ulineær karakter, så systemet udgør et koblet ulineært problem. I denne ph.d. afhandling, er det ulineære problem løst med analytiske metoder og en dynamisk respons på resonans regionen er analyseret ved hjælp af "method of multiple scales". I systemet med mange frihedsgrader er en modal interaktion undersøgt. Virkemåden er blevet identificeret og en diskussion om kontrol er præsenteret. Parametrene for regulatoren er undersøgt ved hjælp af eksperimenter. En vibrationreduktion og frekvensreduktion er identificeret.

Table of contents

Nomenclature

Acronyms

2DOF	Two degree of freedom (system)
APC	Adaptive-passive control
AVC	Active vibration control
EMF	Electro-motive force
FRF	Frequency response function
PD	Proportional-derivative control strategy
RL	(Electrical circuit with) resistance (R) and inductance (L)
SAVC	Semi-active vibration control
SDOF	Single degree of freedom (system)
WoS	Web of Science (`www.webofknowledge.com`)

Symbols

B	Magnetic field density	[T]
B_C	Magnetic field density of the iron core	[T]
B_g	Magnetic field density of the air gap	[T]
C_0	Electro-magnetic parameter	[m]
C_e	Electro-magnetic parameter	[N m^{2}A^{-2}]
c_S	Damping coefficient	[N s/m]
e_f	Voltage drop due to coupling field	[V]
F	Excitation force	[N]
F	Mechanical force	[N]
F_m	Electro-magnetic force	[N]

H	Magnetic field intensity	[A/m]
h	Total air gap	[m]
h_0	Initial air gap	[m]
H_C	Magnetic field intensity of the iron core	[A/m]
H_g	Magnetic field intensity of the air gap	[A/m]
h_{st}	Static deflection	[m]
i	Electric current	[A]
i_{DC}	DC current	[A]
$i_{DC,l}$	Limiting DC current	[A]
i_e	Loss current	[A]
i_m	Magnetizing current	[A]
k_S	Stiffness coefficient	[N/m]
L	Length of magnetic flux path	[m]
L	Inductance	[H]
l_C	Equivalent magnetic flux path in the iron core	[m]
l_g	Equivalent magnetic flux path in the air gap	[m]
L_l	Leakage inductance	[H]
l_l	Equivalent leakage magnetic flux path	[m]
J_0	Mass moment of inertia	[kg m^2]
m_m	Mass	[kg]
N_w	Number of turns of a coil	[-]
R	Electrical resistance	[Ω]
R_e	Equivalent loss resistance	[Ω]
R_S	Equivalent resistance	[Ω]
S_C	Equivalent cross-section of the iron core	[m^2]
S_g	Equivalent cross-section of the air gap	[m^2]
t	Time	[s]
u	Electric voltage	[V]

u_{DC}	DC voltage	[V]
u_i	Induced voltage	[V]
w	Deflection due to vibration	[m]
W_E	Electric energy	[J]
W_e	Energy transferred to the coupling field by electric system	[J]
W_f	Energy stored in the coupling field	[J]
W_M	Mechanical energy	[J]
W_m	Energy transferred to the coupling field by mechanical system	[J]
x_S	Translation of 2DOF mechanical system	[m]

GREEK SYMBOLS

λ	Magnetic flux linkage	[Wb]
μ_0	Permeability of free space	[T m/A]
μ_{rC}	Relative permeability of the iron core	[-]
Φ	Magnetic flux	[Wb]
Φ_l	Leakage magnetic flux	[Wb]
Φ_m	Magnetizing magnetic flux	[Wb]
$\Re_a$	Air gap reluctance	[H^{-1}]
$\Re_c$	Iron core reluctance	[H^{-1}]
$\Re_l$	Leakage reluctance	[H^{-1}]
θ_S	Rotation of 2DOF mechanical system	[rad]

Thesis Details

Thesis Title:	Semi-active vibration control by means of electromagnetic elements
Ph.D. Student:	Radoslav Darula
Supervisor:	Prof.Sergey Sorokin Dept. of Mech. and Manuf. Eng., Aalborg University

The main body of this thesis is composed of the following papers:

- **Paper A**
  Darula, R., Stein, G. J., Sorokin, S., 2011: *An Application of Electromagnetic Induction in Vibration Control*. In Marvalova, B, et al.: Proceedings of the 10th biennial International Conference on Vibration Problems ICoVP 2011, Prague. Liberec, CZE: Technical university of Liberec, Springer Proceedings in Physics, Volume: 139, Pages: 447-453 , ISBN: 978-94-007-2068-8. DOI: 10.1007/978-94-007-2069-5_61.

- **Paper B**
  Darula, R., Sorokin, S., 2012: On non-linear dynamics of a coupled electromechanical system. *Nonlinear Dynamics*. Vol. 70, No 2, p. 979-998. DOI: 10.1007/s11071-012-0505-0.

- **Paper C**
  Darula, R., Sorokin, S., 2013: *An Analytical Study of Non-Linear Behaviour of Coupled 2+2x0.5 DOF Electro-Magneto-Mechanical System by the Method of Multiple Scales*. In Rustighi, E., et al.: RASD 2013, 11th International Conference Recent Advances in Structural Dynamics, July 1-3. Pisa, IT. p.841.1-841.12. ISBN: 978-08-543-2964-9.

- **Paper D**
  Darula, R., Sorokin, S., 2014: Analysis of Multi-Physics Interaction Effects in a Coupled Dynamical Electro-Magneto-Mechanical (2+2x1/2)DOF system. *Journal of Sound and Vibration*. Vol. 333, Issue 14, p. 3266-3285. DOI: 10.1016/j.jsv.2014.03.006.

- **Paper E**
  Darula, R., Stein, G.J., Kallesøe, C. S., Sorokin, S., 2012: *Mathematical Modelling and Parameter Identification of an Electro-Magneto-Mechanical Actuator for Vibration Control*. In Bernard, A., et al.: ASME 2012 11th Biennial Conference on Engineering Systems Design and Analysis (ESDA2012), Vol. 2, July 2-4, 2012. Nantes, FR: ASME, 2012. p. 291-300. ISBN: 978-0-7918-4485-4. DOI:10.1115/ESDA2012-82167.

In addition to the main papers, the PhD project was disseminated also in the following papers:

- **Darula, R.**, Stein, G.J., Sorokin, S., 2013: Numerical simulations of electromagnet exposed to vibration. *Engineering Mechanics*. Vol. 20, No. 6, p. 439-448.
- Stein, G. J., **Darula, R.**, Sorokin, S., 2012: *Control of forced vibrations of mechanical structures by an electromagnetic controller with a permanent magnet*. In Sas, P., Moens, D., Jonckheere, S.: ISMA 2012, International Conference on Noise and Vibration Engineering, September 17-19, 2012. Leuven, BEL. p. 385–393. ISBN: 978-90-738-0289-6.
- Stein, G.J., **Darula, R.**, Chmurny, R., 2011: The Limits of the beam sag under influence of static magnetic and electric force. *Engineering Mechanics*. Vol. 18, no. 5/6, p. 323-329.
- Stein, G. J., **Darula, R.**, Sorokin, S., 2011: *Control of transversal vibrations of a clamped-clamped beam by a permanent magnet and a shunt circuit*. In EURODYN2011: Proceedings of the 8th International Conference on Structural Dynamics, July 4-6, 2011. Leuven, BEL: Katholieke Universiteit.
- **Darula, R.**, Sorokin, S., Stein, G. J., 2011: *Numerical Simulations of Electromagnet Exposed to Vibration*. In: Nahlik, L., et al. Applied Mechanics 2011: Proceedings of 13th Conference AM2011, April 18-20, 2011. Brno, CZE: Institute of Physics of Materials, Academy of Sciences of the Czech Republic. p. 31-34. ISBN: 978-80-87434-03-1.
- **Darula, R.**, 2011: *Solving Electro-Magneto-Mechanical Coupled System by Means of Method of Multiple Scale*s. In: DCAMM 2011: 13th Internal Symposium, Vejle, March 14-16, 2011. Poster. Copenhagen, DK: DTU.
- **Darula, R.**, Sorokin, S., 2010: *Mathematical Modeling of a Semi-Active Vibration Controller with Electromagnetic Elements*. In: ERICSSON, A. and TIBERT, G. 23rd Nordic Seminar on Computational Mechanics. Proceedings of NSCM-23, October 21-22, 2010. Stockholm, SWE: KTH Mechanics, p. 93-96. ISSN: 0348-467X.

This thesis has been submitted for assessment in partial fulfillment of the PhD degree. The thesis is based on the submitted or published scientific papers which are listed above. Parts of the papers are used directly or indirectly in the extended summary of the thesis. As part of the assessment, co-author statements have been made available to the assessment committee and are also available at the Faculty.

Preface

The PhD thesis has been submitted to the Faculty of Engineering and Science in a partial fulfilment of the requirements for obtaining the PhD degree in Mechanical Engineering. The presented work has been carried out at the Department of Mechanical and Manufacturing Engineering during a period from September 2010 to September 2013 under a supervision of prof. Sergey Sorokin.

The PhD project was solved as a work package of a Danish-Swedish EU InterReg IV-A - Silent Spaces project, focused on reduction of sound and vibration originating also from mechanical devices/structures to a civil engineering structures.

The thesis is written as a collection of peer-reviewed papers and conference articles aided with a summary of concepts and measurement results.

During the PhD study, number of people helped me to move on with the project and I would like to express my gratitude to all of them. Especially, I would like to thank my main supervisor prof. Sergey Sorokin for all his time, patience and aid during all three years of the project as well as to industrial partners Jan Balle Larsen, Carsten Skovmose Kallesøe, Thomas Hørdum Sørensen, from Grundfos for all their time and consultations. Also many thanks my parents giving me an opportunity to start a study in Aalborg and for all their support. A great help and support in a lab was provided by Steen Holmgaard, Grundfos. Also without Søren Erik Bruun from a DMME AAU workshop the experimental demo set-ups would not be feasible to be created. Special thank I am expressing Bruel&Kjaer (namely Tom Sørensen and Peter Lund) for all the support to B&K equipment, software and licensing. Our charming secretaries help to fight with all that papers, forms and other (non-academic) tasks, and I would like to express my big thank them. I would like to thank also Dr. G.J. Stein, DMMM Slovak Academy of Sciences, for cooperation during the first stage of the project and my thanks goes also to all the others who helped me to move on with the project and/or to survive (Maz, Alf, sis' Hanka, my bikes, SAAB, Atlantic ocean I used to escape to...).

Radoslav Darula
Aalborg University
June 17, 2014

1 Introduction

1.1 Background and motivation

Vibration (or sound, which in fact is vibration of air particles), is around us from very early beginning of mankind, or to be more precise, from the very beginning of the Earth. However, as sketched in Fig. 1.1, there was no knowledge about vibration at the beginning. People had different, more important troubles to solve. Rao in his textbook (Rao, 2004) dates the analysis of vibration back to 4000 B.C., to the investigation of musical instruments. Other field, which had initialized the investigation of vibration, was a study of earthquakes and development of seismographs (in China A.D. 132).

And then there was a heroic era of giant steps in understanding of vibration and dynamics in general, thanks to Galileo Galilei, Sir Isaac Newton, Daniel Bernoulli, Joseph Lagrange, Charles Coulomb, G.R. Kirchhoff, Lord Baron Rayleigh and many others.

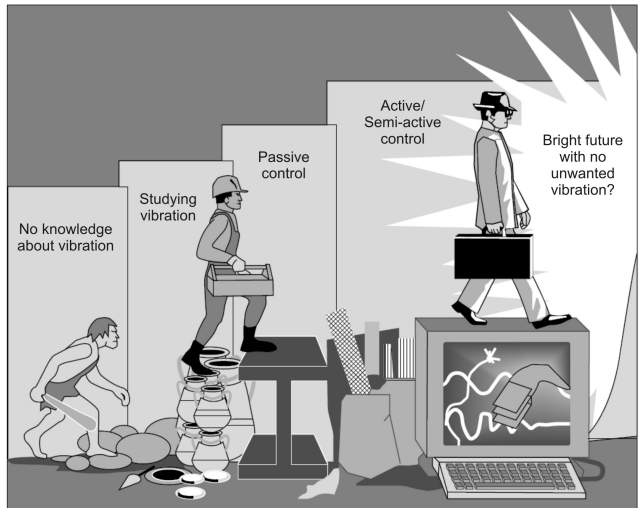

Figur 1.1: Eras of vibration study and control (figure modified from (Schwartz, 2002))

Understanding vibration (and so the sound) was a very important step towards its control. Firstly, just passive elements were implemented. Rubber, wood, or coil/leaf springs can be found in various old machines to solve the problem of excessive vibration.

However the passive way of control had a big drawback. It was effective only for some specific operation conditions. And cars, planes, or other machines started to operate at various speeds. So a development of controllers moved on towards devices allowing to change their properties and the era of active/semi-active devices has started. Further discovery of smart materials, improvement of computer technology spun off a process of optimization of control strategies and now the machines can be controlled virtually on-line and adjust their properties continuously.

And what will be next? Well, hopefully a bright future of silent (non-vibrating) machines will come soon and we will enjoy that sound of silence.

There is still quite a long way to reach this goal, but to contribute with a small step, this PhD project was proposed and done. We have selected the field of a semi-active control, where we decided to specialize on a particular controller, an electromagnetic element. The aim of the project, and so of the thesis, is to provide a theoretical background and basic understanding of the physics behind the control process, its operation and to analyse its non-linear regimes (to be avoided in practical applications). It is not a giant leap done, but hopefully at least it is a small step towards a silence.

1.2 PhD project objectives

The aims of this PhD project can be summarized into following bullets:

- **Analysis of a dynamical response of the electromagnet exposed to vibratory motion** - with a focus on a process of electromagnetic induction and dissipation of energy.
- **Investigation of electromagnet's equivalent damper or/and spring properties** - searching for controller's operation regions.
- **Formulation of a mathematical model** - including mechanical, magnetic and electric behaviour of the system. Considering energy losses based on experimental observations. The formulations in linear and weakly non-linear domains are of interest.
- **Experimental identification of parameters** - identification of the electromagnetic parameters in particular.
- **Solving the coupled problem in time and/or frequency domain** - analysis of the linear and weakly non-linear models derived using analytical/numerical tools.
- **Analysis of the non-linearities in the system using analytical tools** - implementation of the analytical mathematical tools to understand non-linear behaviour of the system.
- **Perform a parametric study of the controller** - investigation of the influence of key parameters on performance of the controller.

- **Prototyping** - demonstration of the controller's operation on a practical, real-life example.

1.3 Structure of the thesis

The thesis is written as a collection of papers, where two journal articles, published in well recognized peer-reviewed journals indexed in WoS as well as Scopus, are supplemented with three articles presented at distinguished international conferences and published in peer-reviewed proceedings (where one conference paper (ICoVP 2011) is indexed in WoS and another one (ESDA 2012) in Scopus). The third article was presented at a well established conference (RASD 2013) organized by one of leading institutes in a field of sound and vibration - ISVR Southampton, UK and the paper in the proceedings was also subjected to a strict peer-review process.

The full references to the papers together with abstracts are attached at the end of the thesis. They are labelled in a sequence of their citation in the text and cover following subjects:

Paper A (Darula et al., 2011)

- The paper presents a general concept of the controller and a simplified linearised model is derived.
- In order to simplify the equations, to generate the magnetic field, a permanent magnet is used instead of a voltage power supply (which is used in experiments). This simplification does not violate a concept of the controller. On the contrary, it helps to generalize the model approach.
- The operation regimes of the vibration controller are identified from the linearised model.

Paper B (Darula and Sorokin, 2012)

- The paper is focused on an in-depth analysis of the non-linear operation of the controller.
- A (1+1/2)DOF electro-magneto-mechanical system is modelled in a non-dimensional form.
- The linearised model is used to identify the natural frequency estimates, used for evaluation of non-linear model implementing a method of multiple scales.
- An electromagnetic damping as well as detuning of the natural frequencies are expressed in an analytical form.
- The non-linear regime (softening) is searched by means of method of multiple scales.

- Stability analysis of the frequency response of the non-linear system is performed.
- The limit and backbone curves are identified and a parametric study on non-linear response is done.
- A virtual experiment (using MATLAB Simulink environment) is performed to validate the analytical (multiple scales) model.
- A discussion on a de-coupled system (where the non-linearities are most pronounced) is presented.

Paper C (Darula and Sorokin, 2013)

- A 2DOF system with two electro-magneto-mechanical couplings compose a (2+2x1/2)DOF problem analysed in the paper.
- The coupled set of equations describing the system's dynamics is derived.
- The static analysis is performed and limit points are identified.
- Eigenvalue analysis is done and detuning of natural frequencies is searched.
- An analysis of the non-linear regime is restricted to a primary resonance analysis of a fully de-coupled system, where the softening behaviour is observed for both modes of vibration.
- A brief analysis of the electrically de-coupled system with a parametric study is presented.
- Validation of the analytical results by means of a numerical experiment (MATLAB Simulink model) is used to verify correctness of the analytical model.
- Parametric study is performed on a fully de-coupled system, i.e. system with most pronounced non-linearities.

Paper D (Darula and Sorokin, 2014)

- The concept of (2+2x1/2)DOF system introduced in paper C (Darula and Sorokin, 2013) is analysed more deeply focusing on modal interactions.
- The governing equations are derived for three cases of a physical domain coupling: (a) linear system; (b) mechanical system with magnetic non-linearities; (c) fully coupled system.
- The linear system is used for eigenvalue analysis.
- From the eigenvalue problem the operation regimes (affecting the natural frequencies) are presented.
- The non-linear system is analysed, where on a top of a primary resonance

analysis of a fully de-coupled system and basic analysis of a sub-harmonic excitation of an electrically de-coupled system presented in paper C (Darula and Sorokin, 2013), the internal parametric resonance is done.

- The uni- and bi-modal response is presented and a stability analysis as well as a parametric study is performed. The numerical simulations (using MATLAB Simulink model) proved the analytical outcomes.
- Equivalent linearised model is derived and compared with the non-linear one in order to search for regions where the linearised model provides sufficient estimation.
- An in-depth discussion on operation regimes of the coupled electro-magneto-mechanical system is presented.

Paper E (Darula et al., 2012)

- The (1+1/2)DOF model is used to analyse the losses introduced by an electro-magnetic circuit.
- The experimental set-up used for investigation is presented.
- Models of the losses are derived in an analytical form (a lumped parameter approach is used) and parameters are identified experimentally.
- The losses are assessed and the models are verified.

2 State-of-the-art

The vibration control of machines and/or structures is a subject, treated in innumerable textbooks and articles. A brief review of the general concepts, focused on state of the art in the field of semi-active control strategy of heavy machinery and/or structures and implementation of electromagnetic forces in the vibration control is presented in this section.

2.1 Vibration control strategies

From the view point of strategy to treat the excessive vibration, one can distinguish following cases (de Silva, 2007; Rao, 2004):

- **Vibration isolation** - i.e. to isolate (reduce transmission) the source from the protected system/environment.
- **Introducing damping / energy-dissipating mechanism** - to remove/-dissipate the energy from the system.
- **Vibration absorption** - a secondary mass-spring-damper system (an vibration absorber/neutralized) is added to protect the host structure from vibration.
- **Vibration control** - a driving force/torque applied from an external device, the force can be altered to adjust for actual conditions (so-called motion tracking) and so avoid operation at resonance.

The main classification of the vibration control strategies from the view point of adjustment of controller's properties, according to (Casciati et al., 2006; de Silva, 2007; Fuller et al., 1997; Saeed et al., 2013), include:

- **Passive** - which are capable to dissipate part of input energy, but no adjustment of their properties is possible. On the other hand it means, that they are inherently stable, do not require any external energy and are of a relatively simple design and construction.
- **Active / Fully-active** - have an ability to automatically supply a force into the structure to counteract the unpredictable vibrations. They require

significant energy to perform the control and the systems are complicated, even they can become unstable in some operation regimes. For their operation they require an actuator, electronic controller and sensor.

- **Semi-active / adaptive-passive** - are essentially passive elements capable to store or dissipate energy. They are able to adjust their properties (stiffness or dissipative ones) with no control force directly applied to the structure. They include adaptive systems and contain, similarly to the active controllers a sensor, control computer, control actuator. However they operate in switching regimes (i.e. they are activated when it is required). As a downsize, they provide a limited control capacity. On the other hand, they are less power demanding.
- **Hybrid** - the passive, semi-active and/or active control devices grouped into series or in parallel to select the best advantage of each type. The passive components help to keep the controller within performance range, while active ones are responsible for adjustment of its response.

From the view point of a control signal following categories are defined (de Silva, 2007; Fuller et al., 1997; Inman, 2006):

- **Open-loop control / Feed-forward** - the strategy does not depend on information about the response. The systems get information about the excitation, where this information is fed-forward to the actuator.
- **Closed-loop control / Feed-back** - the strategy depends on information about the response - when the information about the excitation is not known, the excitation is measured by a transducer and a control signal containing information about the source is fed back to the actuator.

2.2 Variable stiffness elements

Focusing on a vibration control which allows an alternation of system's stiffness (and thus the natural frequency is effectively controlled), following approaches are presented in surveys (Brennan, 2006; Casciati et al., 2006):

- **Geometrical/shape control** - which can be reached by a change of an active number of coils (Franchek et al., 1996) or in a case of leaf springs by a variation of a gap between beams (i.e. beams separation). Another way to modify stiffness by a control of geometry is to alter the curvature of a beam (Brennan, 2006).
- **Shape memory alloy** - is a special type of so-called smart material, which modifies its mechanical properties (Young's modulus) when exposed to variation of temperature.
- **Magneto/electro-sensitive material** - the stiffness changes by an application of the magnetic/electric field to the magneto/electro-sensitive material (e.g. fluid or rubber). A beam with a variable stiffness ensured by a

magneto-rheological fluid filling the beam is presented in (Brennan, 2006). An implementation of magneto-sensitive rubber in a reduction of structure-borne sound is analysed in (Kari and Blom, 2005), where the material used provides alternation in shear modulus and even some additional losses (i.e. damping as well) are introduced changing magnetic field.

- **Electro-magnetic elements** - where the electromagnet is integrated in the vibratory system. The electro-magnetic force is inversely proportional to the displacement, which means that the elements behave as 'negative' springs (i.e. they are reducing the stiffness). The vibration isolation implementing this concept is discussed e.g. in (Hoque et al., 2012; Mizuno et al., 2007).

2.3 Variable dampers

Among devices allowing variation of their energy dissipation properties, one can list (Casciati et al., 2006; de Silva, 2007):

- **Variable rate dampers** - a hydraulic piston with adjustable orifice is used to control a flux of the fluid and thus to control a level of viscous damping (Karnopp et al., 1974).
- **Friction dampers** - the level of damping force (energy dissipation) can be controlled e.g. by means of a control of joint's clamping. In (Nitsche and Gaul, 2002) a piezoelectric disk is used as a washer.
- **Electro/magneto-rheological dampers** - are an example of a viscous dampers that allow to change a viscosity of a fluid by a variation of the electric or magnetic field.
- **Eddy current dampers** - when a variable magnetic field is applied to a ferromagnetic material, eddy currents are induced in a material and vibration energy is dissipated.

2.4 Electro-magneto-mechanical devices

The electro-mechanical devices are combining three physical domains which can be viewed as three subsystems (Furlani, 2001): (a) electrical circuit; (b) electro-mechanical coupling; (c) mechanical subsystem, where the interaction between the subsystems is presented in Fig. 2.1.

A typical electro-mechanical device is composed as shown in Fig. 2.2: a coil

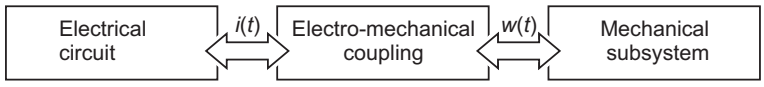

Figur 2.1: A sketch of an interaction within in electro-magneto-mechanical device with electric current $i(t)$ and mechanical displacement $w(t)$

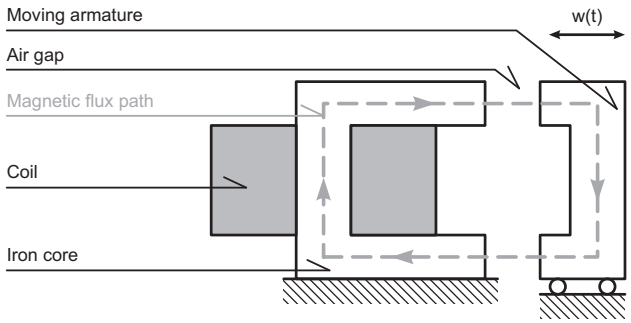

Figur 2.2: A sketch of the electro-magneto-mechanical device

which generates the magnetic field, an iron core and moving armature to guide the field as well as an air gap between the core and armature to ensure a variable reluctance (and so a variable magnetic field).

2.4.1 Modelling of electro-magneto-mechanical systems

In many engineering applications, to analyse the system with a simple geometry, a lumped parameter approach in modelling can be used, i.e. the electrical circuit can be expressed in terms of an equivalent source, a resistance, an inductance and a capacitance, the magnetic circuit in terms of an equivalent reluctance and a magnetomotive force and the mechanical subsystem using lumped mass, damping, stiffness and external excitation force (Bishop, 2002; Fitzgerald et al., 2003; Furlani, 2001; Krause and Wasynczuk, 1989).

Furthermore, if the device is operated in low-frequency regime, the effect of capacitance can be neglected. Then the electrical circuit is modelled as an RL circuit (i.e. a system with equivalent resistance and inductance).

2.4.2 A half degree of freedom

The electrical system, modelled as the RL circuit, is mathematically expressed by a differential equation of the first order. This can be viewed from a mechanical view point as an equivalent mechanical system with stiffness and damping element (Fig. 2.3b), which is identified as a half degree of freedom system (Andronov et al., 1959; Panovko and Gubaniva, 1987). This notation is used in the thesis.

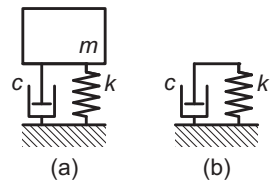

Figur 2.3: (a) SDOF mass-spring-damper system; (b) 1/2 DOF spring-damper system, with stiffness k, damping c and mass m

2.4.3 A negative stiffness

As noted in Sec. 2.2, the electromagnetic forces behave as spring restoring forces with a negative stiffness constant. In order to clarify this concept, a sketch of the spring characteristics with a positive (k_p) and a negative stiffness (k_n) are shown in Fig. 2.4. As can be seen, a 'compression' of the device (i.e. a reduction the distance x), increases the restoring force of the negative spring, i.e. it has the opposite behaviour compared with classical (positive stiffness) springs. This is a typical feature of forces induced by an electromagnetic elements.

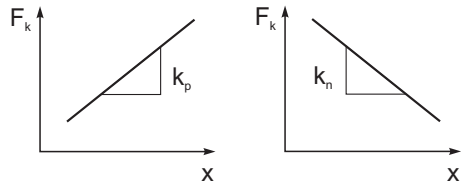

(a) (b)

Figur 2.4: Force-displacement curves for: (a) positive ($F_k = k_p x,\ k_p > 0$) (b) negative stiffness ($F_k = k_n x,\ k_n < 0$)

2.4.4 Losses in the electro-magneto-mechanical systems

In the electro-magneto-mechanical systems operating at low frequencies, one can distinguish following types of losses, which are associated with ferromagnetic materials (Krause and Wasynczuk, 1989; Mohan et al., 1995):

- **Leakage inductance** - if the magnetic flux is not completely linked to the coil (e.g. if winding is not coupled tightly to the core), additional flux is generated.
- **Hysteresis losses** - losses due to alignment of the magnetic domains in the material.
- **Eddy current losses** - occurs in solid cores made of ferromagnetic materials due to variation of magnetic flux.

From the view point of control of losses, the leakage inductance is dependent on geometry of electromagnet's ferromagnetic core and electrical coil. Thus their proper design can reduce (or increase) the amount of energy dissipated in this way. Hysteresis losses are directly linked to the core's material and can be altered changing the material properties. The reduction of the eddy current losses is possible using e.g. laminated core.

2.4.5 Electromagnets in vibration control

Utilization of the electromagnetic force for various industrial applications (also related to vibration control) is not something, which has emerged recently. The research has been conducting for quite some time. Well known applications of

electromagnetic forces in vibration control are e.g. in MAGLEV trains (Bishop, 2002) or for magnetic bearings (Chiba et al., 2005).

As noted in (Behrens et al., 2003), the electromagnetic controllers provide larger control force, longer stroke, are non-contact and more robust than e.g. piezoelectrics. Therefore they are suitable for industrial applications.

The way to utilize the electromagnets in vibration control can be summarized as follows:

- **Passive elements** - with no ability to alter their dynamical properties (e.g. stiffness or dissipative ones)
  - **Eddy current dampers** - the eddy currents emerge when the alternating magnetic field is applied to a ferromagnetic material. A concept, where using a permanent magnet attached to the free edge of a cantilever beam is presented in (Chakraborty and Tomlinson, 2003). Tonoli et al. (2008) use a pair of electromagnets and a moving mass made of ferromagnetic material. Apart of the damping, they observed a change of natural frequencies, so their concept introduced also a negative stiffness into the system.
  - **Electromagnetic shunt damping** - the concept of shunt damping, i.e. dissipation of energy by means of electric circuit (an electrical impedance), which is widely used in piezoelectric systems, was implemented in (Niu et al., 2009) for an electro-magneto-mechanical device - a cantilever beam with an electromagnet, where the magnetic field is generated by a permanent magnet placed to a frame (i.e. not at the beam to save weight) and due to Faraday's law a current is induced in the coil of electromagnet attached to the beam. The induced current is then dissipated in the shunt.
- **Active elements** - another group summarizes the devices which allow to change its properties, usually using some control (feedback) loop
  - **Eddy current dampers** - are also used as passive elements. But when the permanent magnet is substituted by the electromagnet, the amount of damping can be changed, i.e. an active/semi-active control can be introduced. Some hybrid design, a permanent magnet combined with an electromagnet and adding the control loop to reduce vibration of a slender cantilever beam is analysed in (Sodano and Inman, 2008).
  - **Negative stiffness** - a concept of negative stiffness introduced by an electromagnet was implemented by (Hoque et al., 2012; Mizuno et al., 2007) in a vibration isolation system using a PD control strategy.
  - **Self-sensing** - in order to remove the sensor from a control chain Paulitsch et al. (2006) or Bonfitto et al. (2009) used so-called self-sensing control strategy.

From the view point of types and location of electromagnetic elements, mostly

U-shaped magnets are applied. In some of the design concepts, e.g in (Gospodarc et al., 2007; Li et al., 2012; Tonoli et al., 2008) two magnets are implemented. On the other hand in (Daley et al., 2006; Mizuno et al., 2007) a single magnetic element is sufficient.

The operation regimes of electro-magnetic controllers in a frequency domain are analysed e.g. in (Tonoli et al., 2008):

- **Equivalent stiffness range** (below resonance) - the electromagnetic device is acting as a spring element, i.e. introduces negative stiffness.
- **Damping range** (in the vicinity of resonance) - the electromagnetic device behaves as a viscous damper.
- **Mechanical stiffness range** (above resonance) - the electromagnetic device does not influence the dynamic response, i.e. only the passive stiffness controls the response.

2.5 A dynamical response of non-linear systems

As noted in the previous section, the electro-mechanical systems, which utilize the magnetic (or electro-magnetic) force, are inherently non-linear.

In order to solve the non-linear problems, variety of methods (numerical or analytical) can be applied. In the project some numerical simulation using MATLAB Simscape environment was implemented (as summarized in Sec. 4.5). However, the core of the work in the thesis was devoted to the analytical study.

From analytical view point, the perturbation methods are suitable for investigation of non-linear systems. In literature (Hinch, 1991; Nayfeh, 1991; Thomsen, 2004), there can be found number of perturbation methods ready to be applied, such as a method of multiple scales, a method of averaging, a method of time-averaged Lagrangian, etc.

The method of multiple scales, applied in the PhD project, is a method used to solve weakly non-linear systems, excited in a close to resonance region. The method is described in a number of textbooks, e.g. (Hinch, 1991; Nayfeh, 1991; Thomsen, 2004) and it is based on a separation of the the problem into two (or more) time scales describing the dominant (leading order) and weak (modulation) response of the system.

To apply the method of multiple scales, three approaches can be used (Nayfeh, 2000): (a) derivative-expansion; (b) two-variable expansion; (c) generalized. In the thesis the derivative expansion method was chosen as the most optimal. A further discussion on each approach can be found in (Nayfeh, 2000).

One of features of non-linear systems, which is not present in the linear ones is modal interaction, i.e. exciting the system at one mode, other one can be excited as well. The modal interaction in non-linear systems with application of the analytical (perturbation) tools is thoroughly described in (Nayfeh, 2000). An analysis on parametric resonances in systems with magnetic forces using permanent magnets

is presented in (Dohnal, 2007; Schmidt et al., 2007) and they summarize some experimental results in (Dohnal, 2012).

3
Model of the controller

The principle of modelling of the electro-magneto-mechanical vibration control system is presented in this section for a single degree-of-freedom (SDOF) mechanical system coupled to an electrical circuit. This model is used (with necessary variations) in the papers attached to the theses, i.e. in papers A to E.

A 2DOF model was derived for the papers C and D (Darula and Sorokin, 2013, 2014). However, the principle of electro-magneto-mechanical-coupling is exactly the same as in the case of SDOF model, just the mechanical system is coupled to a pair of magnetic and electric circuits. The 2DOF model was chosen to investigate possible modal interactions, as discussed in Chapter 5.

3.1 Definition of terms

If the electromagnet is acting on a suspended mass, as shown in Fig. 3.1, the action of a static force will induce a static deflection. In order to clarify the further derivations let us introduce following quantities:

- **Total air gap** - $h(t)$ - characteristics of the actual air gap reluctance during vibration.

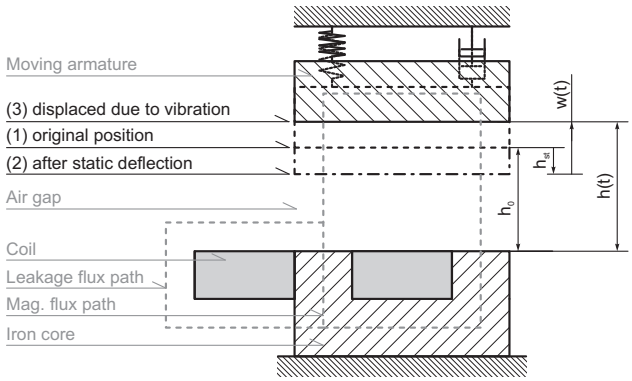

Figur 3.1: Description of the air gap variation

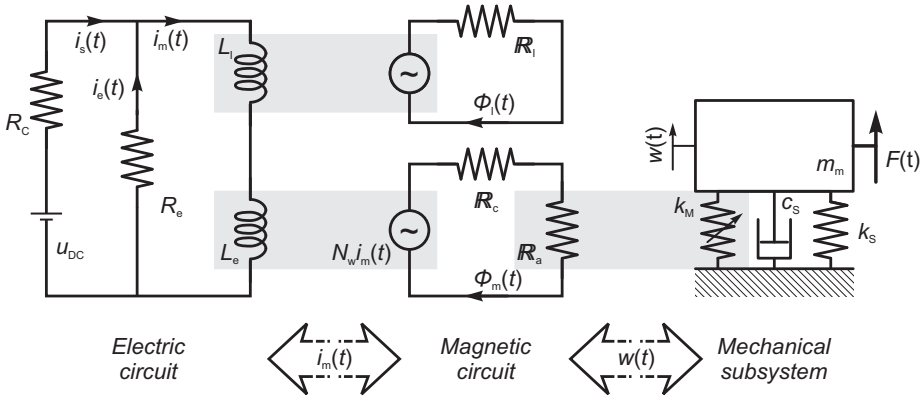

Figur 3.2: Sketch of the sub-models with an indication of the coupling terms

- **Initial air gap** - h_0 - air gap width before the electromagnetic force is applied.
- **Static deflection** - h_{st} - static deflection of the mass caused by static component of electromagnetic force.
- **Deflection due to vibration** - $w(t)$ - deflection of the mass due to action of excitation force. The positive direction is taken upwards, i.e. opposite to the action of electromagnetic force (the force acts downwards in the system presented in Fig. 3.1).

3.2 Coupled electro-magneto-mechanical system

As noted in the Sec. 2.4.1, the electro-magneto-mechanical systems couple three physical domains, where the electric current ($i_m(t)$) and deflection due to vibration ($w(t)$) are the coupling quantities, as indicated in Fig 3.2.

Each of the subsystems will be modelled separately, while in the Sec. 3.2.5 the governing equations are expressed in a coupled form.

3.2.1 Magnetic circuit

First let us start with a magnetic circuit, which binds the electrical system to the mechanical one. More in-depth derivation of the magnetic field is summarized in Appendix A.1.1 and in this section a brief overview is presented.

Using the Ampere's law, a magnetic flux (Φ_m) is expressed as:

$$N_w i_m(t) = H_C l_C + 2H_g h(t) = \frac{\Phi_m(t) l_C}{\mu_0 \mu_{rC} S_C} + 2\frac{\Phi_m(t) h(t)}{\mu_0 S_C} \tag{3.1}$$

$$\Phi_m(t) = \frac{\mu_0 S_C N_w i_m(t)}{l_0 + 2h(t)} \tag{3.2}$$

where $B_C = \mu_0 \mu_{rC} H_C$, $B_C = \mu_0 H_g$ and $\Phi_m(t) = B(t) S_C$, see notations in the beginning of the thesis.

As discussed in Appendix A.1.1, in real systems the leakage flux (a separate magnetic circuit) can model some of the losses in the system. The total magnetic flux in the system is then expressed as a sum of magnetizing (Φ_m) and leakage flux (Φ_l):

$$\Phi(t) = \Phi_m(t) + \Phi_l(t) = \frac{\mu_0 S_C N_w i_m(t)}{\frac{l_C}{\mu_{rC}} + 2h(t)} + l_l i_m(t) \tag{A.5}$$

where the leakage flux $\Phi_l = l_l i_m(t)$ with $l_l = N_w/\Re_l$, $\Re_l$ a leakage reluctance to be determined experimentally.

3.2.2 Electric circuit

When the electromagnet is exposed to vibration (electric reluctance change), voltage is induced in a coil, which is expressed by the Faraday's law (Furlani, 2001):

$$u_i = -N_w \frac{d\Phi(t)}{dt} \tag{3.3}$$

As shown in Fig. 3.2, the equivalent electric circuit consists of a coil resistance R_C, equivalent loss resistance R_e, coil and leakage inductances (L_e, L_l), where R_e and L_l are included to create more general model, which would allow to introduce also the losses in the electro-magnetic circuit.

Derivations of the electric equations are summarized in Appendix A.1.2. Using Kirchhof's current and voltage laws and following the notation in Fig. 3.2, the electrical circuit can be expressed as

$$\begin{aligned} u_{DC} =& R_C i_m(t) + R^* \left(L_l + \frac{2C_e}{(C_0 + w(t))} \right) \frac{di_m(t)}{dt} \\ & - R^* \frac{2C_e i_m(t)}{(C_0 + w(t))^2} \frac{dw(t)}{dt} \end{aligned} \tag{A.16}$$

with a resistance ratio $R^* = \frac{R_C + R_e}{R_e}$ and $L_l = N_w/\Re_l$.

3.2.3 Electromagnetic force

The derivation of the electro-magnetic force, a force which couples the electrical circuit (via an electric current $i_m(t)$) to the mechanical system (via a mechanical displacement $w(t)$) is derived using a co-energy approach and summarized in Appendix A.1.3. The final expression is

$$F_m(t) = \frac{C_e i_m^2(t)}{(C_0 + w(t))^2} \tag{A.43}$$

It can be noticed, that the force is inversely proportional to the deflection $w(t)$, i.e. as noted in the Sec. 2.4, the force is a non-linear function of displacement. Furthermore, it is a quadratic function of current $i_m(t)$, i.e. the electro-magnetic force is a non-linear function of both coupling quantities.

3.2.4 Mechanical system

Considering a SDOF system (Fig. 3.2), the mechanical system is composed of an inertia, damping, stiffness elements and exposed to an action of electromagnetic and excitation forces. Then the governing equation (derived in Appendix A.1.4) becomes:

$$m_m \frac{d^2w(t)}{dt^2} + c_S \frac{dw(t)}{dt} + k_S(-h_{st} + w(t)) = F(t) - F_m(t) \tag{A.44}$$

$$m_m \frac{d^2w(t)}{dt^2} + c_S \frac{dw(t)}{dt} + k_S(-h_{st} + w(t)) + \frac{C_e i_m^2(t)}{(C_0 + w(t))^2} = F(t) \tag{A.45}$$

where $C_0 = f(h_{st})$. The static deflection due to the action of electromagnetic force, h_{st}, needs to be considered, as the magnetic force (expressed by Eq. (A.43)) has also a static component.

3.2.5 Coupled set of equations

The coupled electro-magneto-mechanical system is then expressed by a system of equations:

$$m_m \frac{d^2w(t)}{dt^2} + c_S \frac{dw(t)}{dt} + k_S(-h_{st} + w(t)) + \frac{C_e i_m^2(t)}{(C_0 + w(t))^2} = F(t) \tag{A.45}$$

$$\begin{aligned} u_{DC} =& R_C i_m(t) + R^* \left(L_l + \frac{2C_e}{(C_0 + w(t))} \right) \frac{di_m(t)}{dt} \\ & - R^* \frac{2C_e i_m(t)}{(C_0 + w(t))^2} \frac{dw(t)}{dt} \end{aligned} \tag{A.16}$$

where the coupling is done via the mechanical deflection $w(t)$ and the electric current $i_m(t)$.

3.3 2+2x1/2DOF system

In the papers C and D (Darula and Sorokin, 2013, 2014), the SDOF mechanical system was substituted by a 2DOF system, in order to model more complex machine, or structure and analyse also possible non-linear modal interactions.

The derivation of corresponding governing equations is similar to the one for SDOF system, only the mechanical model is expressed by two independent coordinates - a translation $x_S(t)$ and a rotation $\theta_S(t)$.

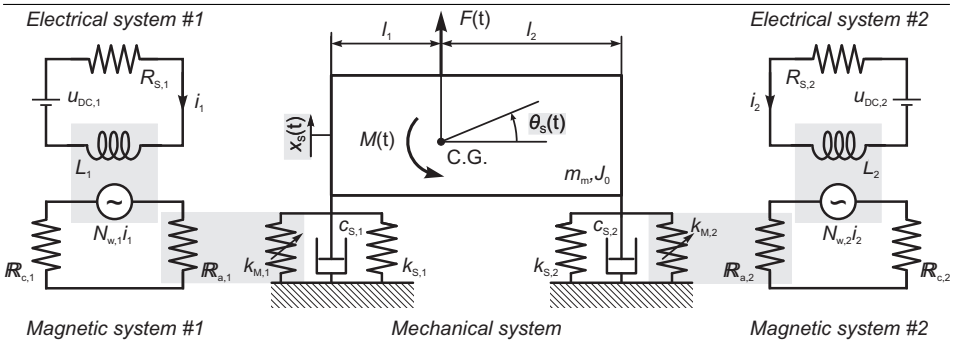

Figur 3.3: Sketch of the (2+2x1/2)DOF electro-mechanical system with an indication of the coupling terms (Darula and Sorokin, 2014)

The coupled system of equation then becomes (Appendix A.1.5):

$$m_m \frac{d^2 x_S}{dt^2} + (c_{S,1} + c_{S,2}) \frac{dx_S}{dt} + (-c_{S,1} l_1 + c_{S,2} l_2) \frac{d\theta_S}{dt} \ldots + (k_{S,1} + k_{S,2}) x_S + (-k_{S,1} l_1 + k_{S,2} l_2) \theta_S + F_{m,1} + F_{m,2} = F \tag{A.50}$$

$$J_0 \frac{d^2 \theta_S}{dt^2} + (-c_{S,1} l_1 + c_{S,2} l_2) \frac{dx_S}{dt} + (c_{S,1} l_1^2 + c_{S,2} l_2^2) \frac{d\theta_S}{dt} \ldots + (-k_{S,1} l_1 + k_{S,2} l_2) x_S + (k_{S,1} l_1^2 + k_{S,2} l_2^2) \theta_S - l_1 F_{m,1} + l_2 F_{m,2} = M \tag{A.51}$$

$$u_{DC,n} = R_{S,n} (i_{DC,n} + i_{AC,n}) \ldots + \sum_{m=0}^{3} \left[(-1)^m \frac{(1+m) C_e}{C_{0,n}} \frac{di_{AC,n}}{dt} (x_S + (-1)^n l_n \theta_S)^m \ldots - (-1)^m \frac{C_e (i_{DC,n} + i_{AC,n})}{C_{0,n}} (x_S + (-1)^n l_n \theta_S)^m \left(\frac{dx_S}{dt} + (-1)^n l_n \frac{d\theta_S}{dt} \right) \right] \tag{A.53}$$

with $n = 1..2$ indicating the number of electro-magnetic circuits, electric current $i_n = i_{DC,n} + i_{AC,n}$ and magnetic forces $F_{m,n} = f(x_S, \theta_S, i_n)$ defined by Eq. (A.43).

4

Semi-active vibration control strategy of the device

In the chapter a discussion on vibration control strategy of the electromagnetic elements is presented. The linearised model is used to identify the controller's operation regimes and numerical simulations (using MATLAB Simscape environment) to analyse the dynamical response at the regimes and investigate an initialization of the controller.

4.1 Static limits

A static deflection (h_{st}) as a function of mechanical stiffness (k_S) and electromagnetic properties can be expressed directly analysing the static part of the linearised version of Eq. (A.45):

$$k_S h_{st} = \frac{\mu_0 S_C}{4} \frac{N_C^2 i_{DC}^2}{(l_C + h_0 - h_{st})^2} \tag{4.1}$$

Eq. (4.1) is a cubic function in h_{st}. As analysed more thoroughly in (Stein et al., 2011), there can be found either three real-valued roots, or one real- and two complex-valued roots, where just one real root (in Fig. 4.1 the root 3) is stable.

A point $(1, h_{st,l}/h_0)$ in Fig. 4.1a is of interest from an application view point, since it represents a maximal current/static displacement before the system becomes unstable. The value of critical current $i_{DC,l}$ is found from the double root (a term under square root becomes negative, i.e. the static deflection becomes complex valued, (Darula and Sorokin, 2014; Stein et al., 2011)):

$$i_{DC,l} = \sqrt{\frac{2k_S(2h_0 + C_0)^3}{27C_e}} \tag{4.2}$$

In the unstable regime ($i_{DC}/i_{DC,l} > 1$), the attractive magnetic force is larger than the repelling spring stiffness force, i.e. the armature of the electromagnet is attracted to its core (Fig. 4.1b) and it ends up with a mechanical contact between the armature and core. This is unwanted, as the electromagnet is not capable to

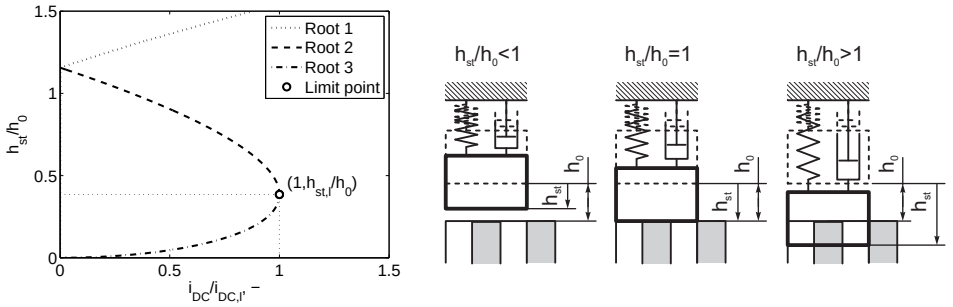

(a) (b)

Figur 4.1: (a) A scaled static deflection as a function of current; (b) visualization of the yoke position for different air gap/static deflection ratios (a physical $h_{st}/h_0 \leq 1$, mechanical contact $h_{st}/h_0 = 1$ and non-physical $h_{st}/h_0 > 1$)

provide neither additional stiffness, nor damping forces. Therefore for an operation of the controller, the value of current needs to be lower than the limit value $i_{DC,l}$.

As the limit current corresponds to the condition expressed by Eq. (4.1), where the electromagnetic force is equal to force exposed by a passive stiffness ($F_m = F_k$), then a case of 'zero stiffness' (Mizuno et al., 2007) is obtained.

The static limits for (2+2x1/2)DOF are discussed in (Darula and Sorokin, 2013), where the limit current is dependent on position of centre of gravity.

Experimental verification of the static displacement estimation as well as limiting point is presented in Sec. 6.2.

4.2 Operation regimes of the controller

Let us first, for simplicity, take a linearised model, i.e. assume that the amplitude of vibration is much smaller than the electromagnetic constant (which is a function of an initial air gap), $w(t) << C_0(h_0)$, and let us expand the electromagnetic force (in a mechanical system) using a power series expansion:

$$F_m(t) = \frac{C_e i_m^2(t)}{(C_0 + w(t))^2} \approx \frac{C_e i_m^2(t)}{(C_0)^2} - 2\frac{C_e i_m^2(t)}{(C_0)^3} w(t) + \mathcal{O}(w^2) \tag{4.3}$$

i.e. we split the force into a static and dynamic (so-called 'negative' stiffness) components.

In paper A (Darula et al., 2011), the operation regimes of the electromagnet (in the paper the permanent magnet was used to generate the magnetic field), operated in a linearised regime, were identified (Fig. 4.2):

- **Passive operation** ($R/L_0 << \omega_a$) - no action of the electromagnet, the dynamical response of the system is fully controlled by properties of a mechanical system.

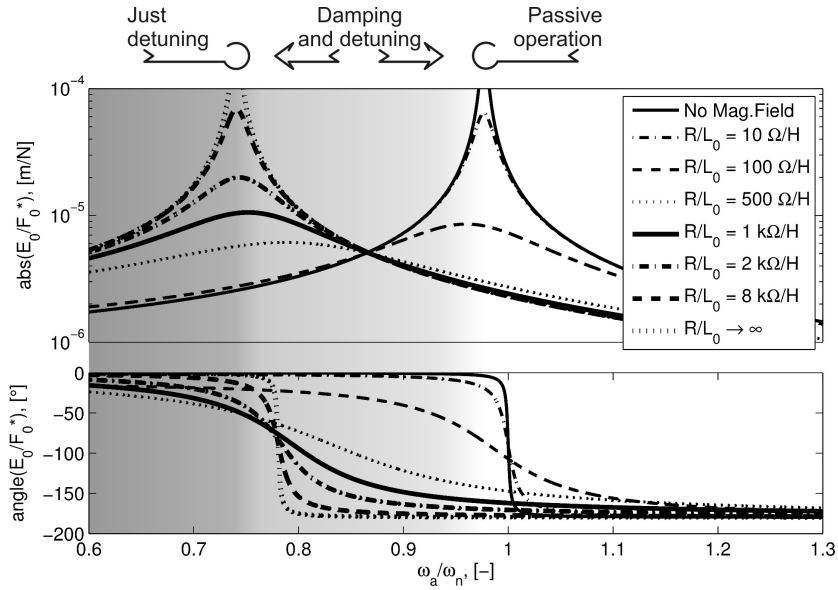

Figur 4.2: Operation regimes of the electromagnetic controller (Darula et al., 2011)

- **Damping and detuning** ($R/L_0 \approx \omega_a$) - the mechanical system is coupled to the electro-magnetic circuit, which introduces to the system a negative stiffness as well as an additional damping. All the modulations are dependent on frequency, as well as on electro-magnetic parameters. Some identification on maximal damping is summarized in paper B (Darula and Sorokin, 2012) and paper E (Darula et al., 2012) and will be discussed in Sec. 4.3.
- **Just detuning** ($R/L_0 >> \omega_a$) - the electromagnet modulates the inertia, as well as stiffness properties and so the maximal detuning (natural frequency change) is obtained. Furthermore, no additional damping from the electro-magnet is obtained, i.e. only a change in resonance frequency is observed.

A more detailed analysis of the regimes for (1+1/2)DOF systems is presented in the paper A (Darula et al., 2011).

From a qualitative view point, the same regimes as for a permanent magnet system were identified also for an electromagnet with a DC power supply (paper B (Darula and Sorokin, 2012)) as well as for a (2+2x1/2)DOF system (papers C and D (Darula and Sorokin, 2013, 2014)), i.e. the discussion on operation regimes can be generalized for any electro-magneto-mechanical system with an electromagnet possessing change of air-gap reluctance and being coupled to an electrical circuit.

4.3 Assessments of detuning and damping

A parametric study on detuning (natural frequency change) and additional (electromagnetic) damping is presented in the paper B (Darula and Sorokin, 2012) for the (1+1/2)DOF system.

Fig. 4.3 shows a variation of the eigenfrequency as a function of electro-magnetic parameters, where κ represents the ratio of a magnetic stiffness (magnetic parameters) and a mechanical stiffness and λ is used to describe properties of an electric circuit. Similar parametric study on detuning for (2+2x1/2)DOF is summarized in the papers C and D (Darula and Sorokin, 2013, 2014).

An expression for an equivalent electro-magnetic damping is derived in the paper as well. The results are presented in Fig. 4.4. and it can be seen, that there is some threshold, where the maximum damping is introduced. This threshold is of interest from application view point.

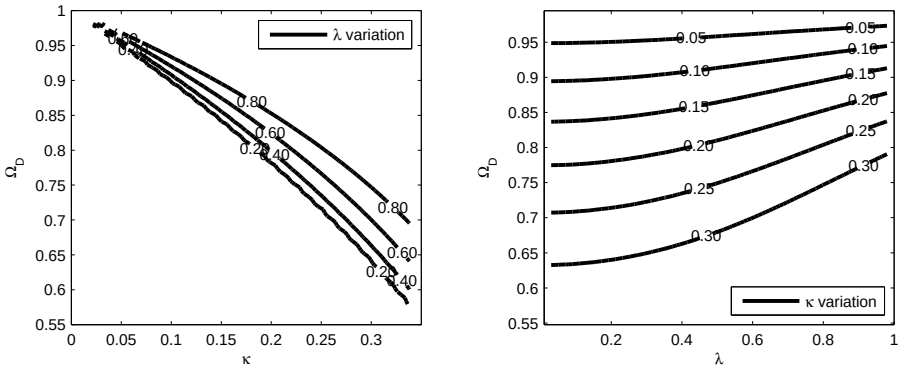

(a) (b)

Figur 4.3: Parametric study on eigenfrequencies Ω_D (Darula and Sorokin, 2012)

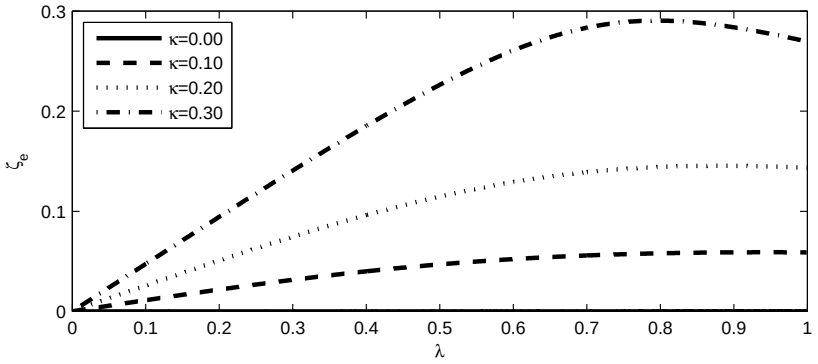

Figur 4.4: Equivalent electromagnetic damping as a function of stiffness ratio (κ) and electromagnetic parameter (λ) (Darula and Sorokin, 2012)

4.4 Discussion on control strategy

The semi-active electro-magnetic controller analysed in the thesis is aimed to operate in so-called switched (on-off) regime, where the properties can be adjusted modifying the electro-magnetic parameters (namely electric current and/or resistance). As shown in Fig. 4.2, three regimes (uncontrolled, damping and detuning) has been identified and depending on the application, the operation in one of the most appropriate regimes can be reached choosing corresponding combination of the parameters of electrical, magnetic and/or mechanical systems.

One of the examples to implement the controller is to use it during a machine start-up. The detuning procedure is sketched in Fig. 4.5, where following stages are recognized:

1. **Machine start-up** (Fig. 4.5a) - the operation speed of the machine is increased, until a frequency Ω_D is reached.
2. **Detuning** (Fig. 4.5b-c) - the electromagnetic element is initialized and negative stiffness introduced, so the natural frequency is reduced (Ω_{nD}).
3. **Reaching the working frequency** (Fig. 4.5d) - the speed is increased further to reach the working frequency Ω_{nO}, where the amplitude of vibration is within limits designed.

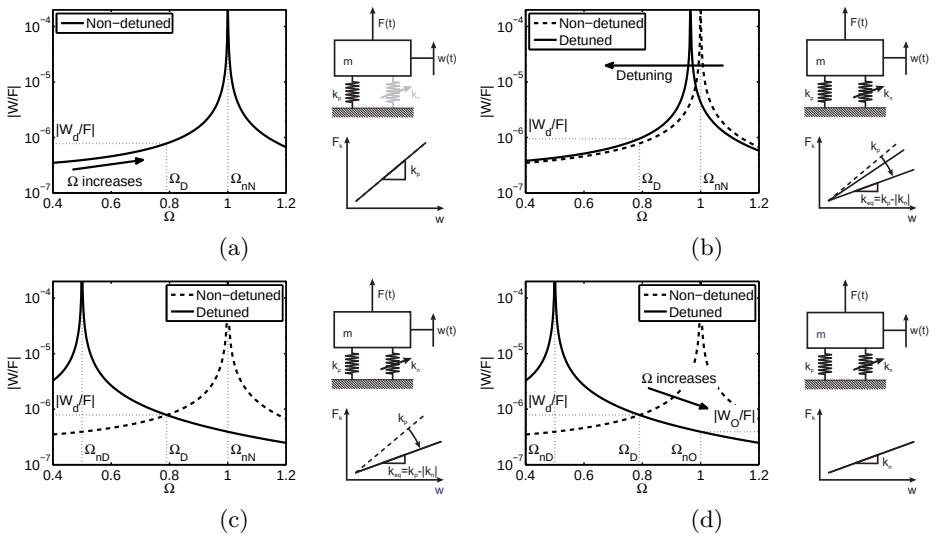

Figur 4.5: Detuning procedure of the controller: (a) machine start-up; (b) natural frequency detuning; (c) reaching detuned natural frequency; (d) reaching working frequency

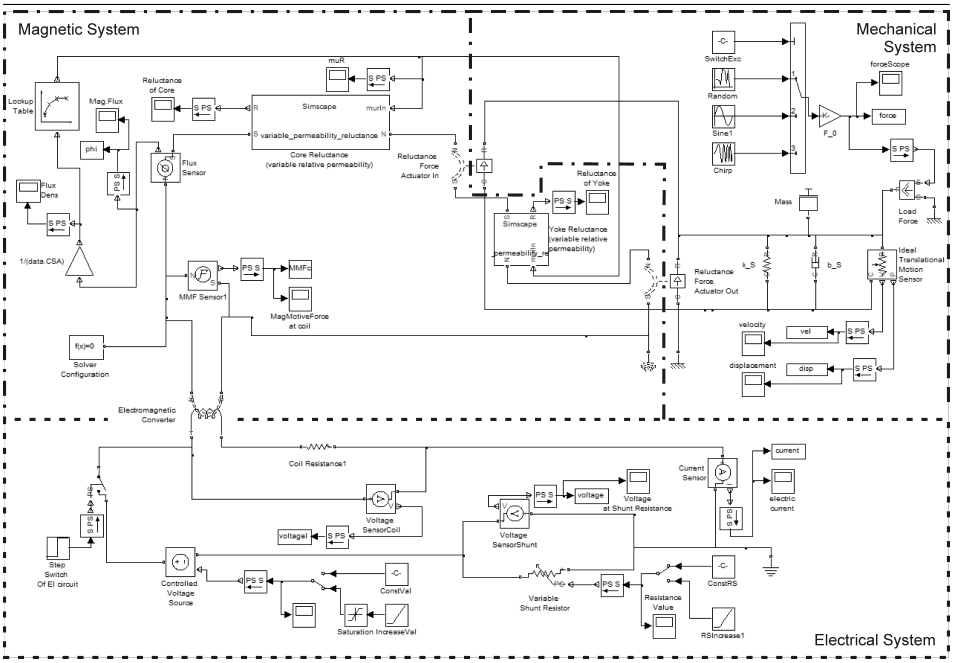

Figur 4.6: MATLAB Simscape model used in numerical study (Darula et al., 2013)

4.5 Numerical simulations

In order to predict the operation of the controller not only in a steady state (i.e. using analytical tools) but also for transients, numerical model was created in MATLAB Simscape environment (Fig. 4.6). A detailed description of the model and results are summarized in (Darula et al., 2013). In this section just the results with a brief discussion are presented.

4.5.1 Identification of operation regimes

Using a random noise excitation, frequency response functions were searched varying the parameters of the electric circuit, which are used to control the properties of the controller (Fig. 4.7).

Fig. 4.7a shows a step-wise increment of supply DC current which is responsible for generation of an electromagnetic force and so reduction of the natural frequency as well as introduction of additional damping.

Furthermore, as the resistance is increased, the regime of detuning and damping ($R_S = 2\text{k}\Omega$), as well as the regime with pure detuning ($R_S \to \infty$) are observed in Fig. 4.7b, as predicted in Sec. 4.2. The comparisons of the Simscape model and analytical calculations (by means of a multiple scales) is presented in papers B and D (Darula and Sorokin, 2012, 2014).

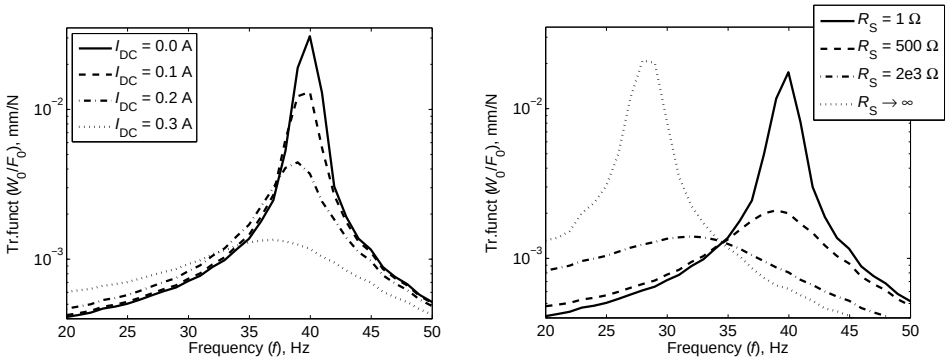

(a) (b)

Figur 4.7: Transfer functions (random noise excitation): (a) variable current (for $R_S = 2\text{k}\Omega$); (b) variable resistance ($i_{DC} = 0.3A \approx 0.7i_{DC.l}$) (Darula et al., 2013)

4.5.2 Initialization of the controller

To analyse the initialization of the controller, two cases are compared in (Darula et al., 2013): (a) a sudden/step introduction of supply current (and so electromagnetic force, Fig. 4.8a and c); (b) a continuous change of the current (Fig. 4.8b and d).

In a case of a sudden switch-on of the controller, very high transient voltages are induced (Fig. 4.8c), which is dangerous from application view point.

In order to avoid these voltage surges a continuous change of the current is used in Fig. 4.8b and d. It can be noticed, that no dangerous voltage peaks occur. As a result of Faraday's law, the induced voltage just follows the vibration.

As compared in Fig. 4.8b and d, increasing the current level, the vibration can be effectively reduced. The rate of change of the current initialization can be adjusted to minimize the operation in resonance region.

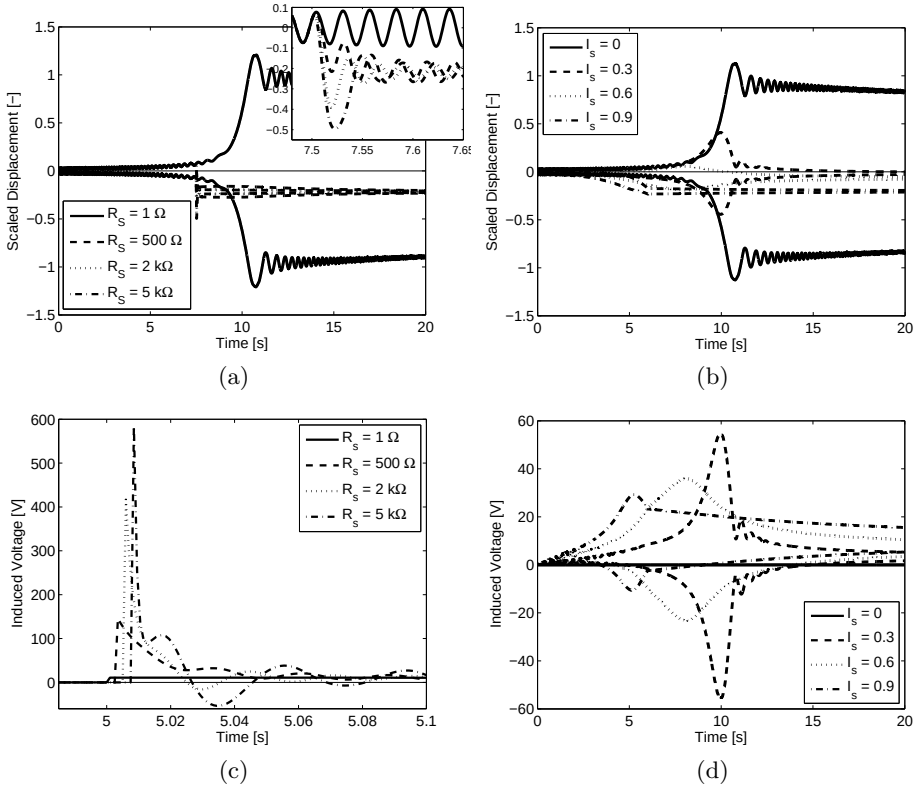

Figur 4.8: Envelopes of vibration amplitudes and induced voltages as a function of time for (a) and (c) sudden initialization; (b) and (d) smooth increase of current (Darula et al., 2013)

5
Non-linear analysis

In most of industrial applications, the linearisation is assumed. However it is important to identify the operation regimes and avoid possible unstable behaviour, which can be introduced by non-linearities.

As defined in Sec. 2.4.2, the electrical system introduces a 'half degree of freedom' (1/2DOF). Therefore for the cases analysed in papers B, C and D (Darula and Sorokin, 2012, 2013, 2014) a notation (1+1/2)DOF and (2+2x1/2)DOF systems is used.

To describe a dynamical response of both types of systems, a model derived in Ch. 3 is employed.

5.1 Method of multiple scales

The non-linear dynamical behaviour of the coupled systems is analysed by means of the method of multiple scales. To apply the method, firstly so-called dominant (leading) terms and weak (modulation) terms need to be identified. In both systems, (1+1/2)DOF as well as (2+2x1/2)DOF, the dominant terms are inertia and stiffness forces, as well as the stiffness component of the electromagnetic force. On the other hand, the weak terms contain damping and excitation forces as well as the damping component of the electromagnetic force. In the electric circuit just the non-linear cross-terms (non-linear terms containing both displacement and current terms) are treated as modulation terms.

Then the two time scales are introduced:

- **Fast time** - to describe the response of a linear system.
- **Slow time** - modulation of this response introduced by non-linearities.

In the analysis of an electric circuit, it is important to split the expression of the current into a real and imaginary parts, where the imaginary one is treated as damping, i.e. classified as a weak term. It means that the coupling of the electric circuit introduces an additional damping. This will be proved in the next sections.

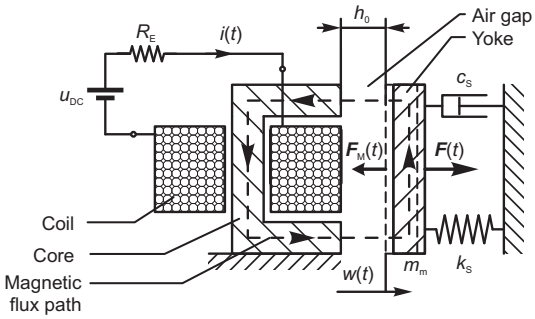

Figur 5.1: Sketch of the (1+1/2)DOF electro-mechanical system analysed in (Darula and Sorokin, 2012)

5.2 (1+1/2)DOF system

In the paper B (Darula and Sorokin, 2012), the non-linear analysis of the (1+ 1/2)DOF system (Fig. 5.1) is summarized. The electric circuit is modelled with no additional losses assumed, i.e. just the equivalent resistance R_E used (no leakage inductance and no additional loss resistance derived in Ch. 3 are considered in the paper).

Since the method of multiple scales, used to evaluate the non-linear response, is valid in a near resonance region, the eigenfrequency analysis needs to be done first. In the paper three approaches are compared, namely using: (a) a linearised system, (b) an expansion of roots of the eigenfrequency equation on the small parameter λ and (c) a method of multiple scales (Darula and Sorokin, 2012).

Solving the eigenvalue problem, three pairs of eigenvalues are found. In order to determine which pair of eigenvalues corresponds to which system (electrical or mechanical), the amplitude ratios are plotted (Fig. 5.2). As concluded in the

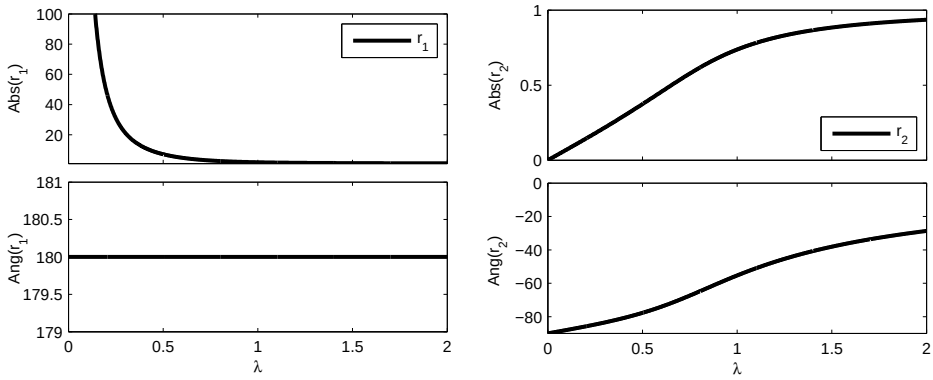

(a) (b)

Figur 5.2: Amplitude ratios and phase shifts for eigenvalues: (a) Ω_{Da1} (controlled by an electric system); (b) $\Omega_{Da2,3}$ (controlled by mechanical system) (Darula and Sorokin, 2012)

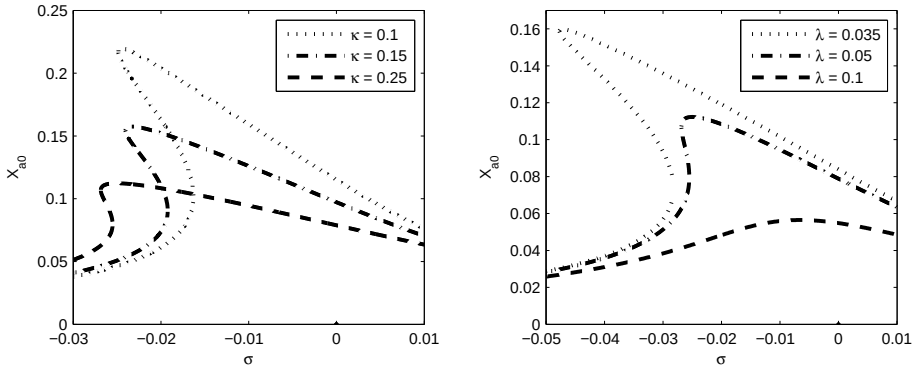

(a) (b)

Figur 5.3: Frequency response functions of displacement amplitudes for: (a) stiffness ratio κ variation; (b) electromagnetic parameter variation (Darula and Sorokin, 2012)

paper, the first pair of eigenvalues is controlled by the electrical system, whereas the mechanical system controls the remaining eigenvalues.

A parametric study of non-linear behaviour is discussed in the paper B (Darula and Sorokin, 2012) as well. Increasing stiffness ratio κ (i.e. introducing a larger electromagnetic force), the effect of non-linearity is enhanced, where the softening behaviour is observed (Fig. 5.3a). On the contrary, the introduction of electrical circuit, i.e. increasing the electromagnetic parameter λ, additional damping is introduced, which smears out the non-linearities.

In the paper B (Darula and Sorokin, 2012) the stability analysis as well as analysis of the backbone and limit curves of non-linear response are analysed.

5.3 (2+2x1/2)DOF system

Adding one more degree of freedom and attaching two controllers, the (2+2x1/2) DOF system was created (Fig. 5.4) and analysed in papers C and D (Darula and Sorokin, 2013, 2014).

The analysis of eigenfrequency is similar to (1+1/2)DOF system. Therefore it is not repeated in this text, it can be found in the papers.

Introducing more degrees of freedom allows us to analyse a modal interactions and possible internal parametric resonances. An introduction to the subject and some results on sub-harmonic excitation are summarized in (Darula and Sorokin, 2013). A thorough analysis of the sub-harmonic excitation with an internal parametric resonance is presented in paper D (Darula and Sorokin, 2014). The regions of uni- and bi-modal response are shown in Fig. 5.5a and b and the jump phenomena is visualized in Fig. 5.5c and d.

In the papers also a parametric study was done in order to find the operation regimes and validation using the numerical model proved the analytical outputs.

Since the results mimic the behaviour of the (1+1/2)DOF model they are not presented here and can be found in the papers.

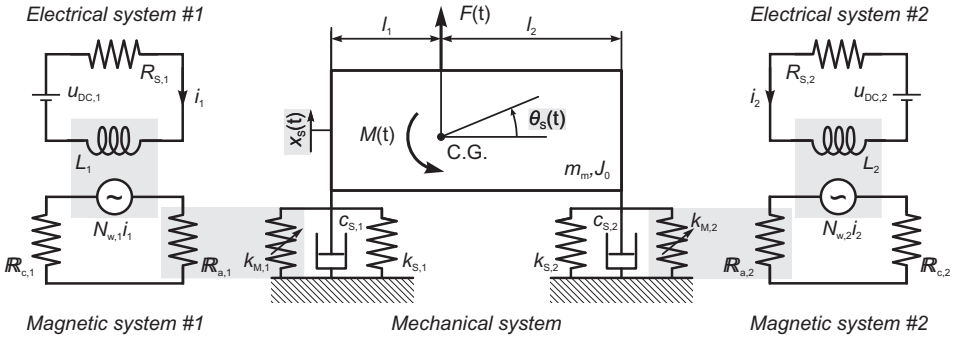

Figur 5.4: Sketch of the (2+2x1/2)DOF electro-mechanical system analysed in (Darula and Sorokin, 2013, 2014)

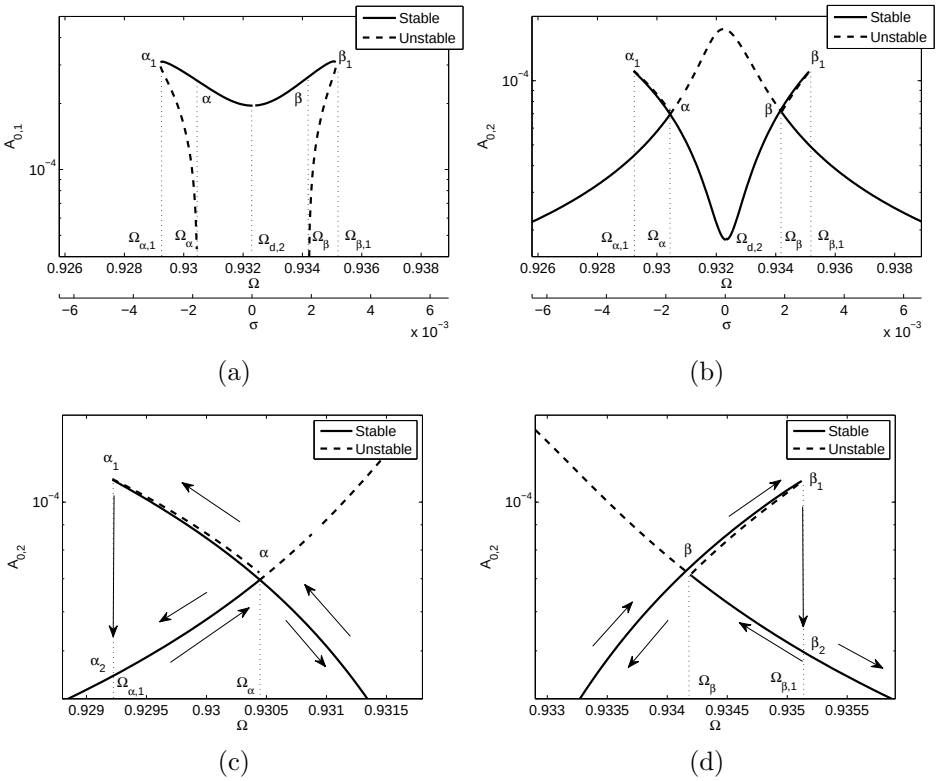

Figur 5.5: Mechanical system with magnetic-non-linearities: (a) indirectly excited mode; (b) directly excited mode; (c) zoom to point α; (d) zoom to point β (Darula and Sorokin, 2014)

6

Experimental characterization & verification of operation

A series of experiments have been executed in order to verify the model and concept of a semi-active (on-off) vibration control scheme based on introduction of the electro-magnetic force and so to alternate the natural frequency and add damping.

A brief overview of the results reported in the paper E (Darula et al., 2012) is presented in the chapter and more detailed discussion on an experimental set-up, apparatus used, as well as some additional information on measurements is summarized in Appendix B.

6.1 Experimental set-ups

Two main set-ups (with some necessary alternations) have been used for measurements. According to their geometry, they are called: (a) a triangular set-up (Fig. 6.1a) and (b) a beam set-up (Fig. 6.1b). Both set-ups were designed to be modular, which allows to modify the properties (stiffness/mass, position of controllers, or type of excitation) and so ensure more versatility in settings of operation conditions.

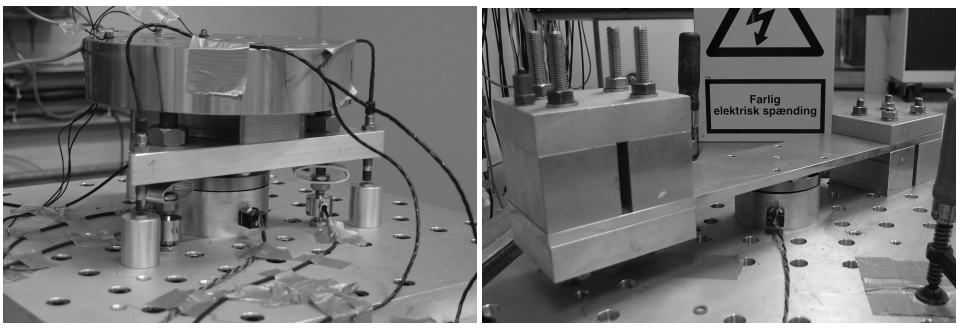

(a) (b)

Figur 6.1: Visulisation of (a) triangular set-up; (b) beam set-up

6.1.1 Triangular set-up

In order to measure also the magnetic force during a vibration, a set-up with serial arrangement of the passive stiffness element and a force transducer was required (Fig. 6.1a). To allow more precise adjustments of the air gap width (and thus magnetic air gap reluctance), a triangular set-up, i.e. support in three points, was designed. It accommodates three force transducers, three displacement transducers, volt- and ammeter directly connected to a data acquisition device (B&K PULSE) to allow time logging of all important quantities.

6.1.2 Beam set-up

The higher stiffness and also more versatile settings of a natural frequency was reached using a clamped-free beam set-up with variable beam thicknesses and end masses.

The controller was intentionally located closer to the clamped end, predominantly to reduce the amplitude of air gap variation. The set-up is built so that in later stage a location of the mass/machine can be varied in order to verify different concepts of controller's position.

6.2 Static measurements

Firstly the static parameters need to be measured in order to identify the elements of the electro-magnetic force as well as coil resistance of the electromagnet.

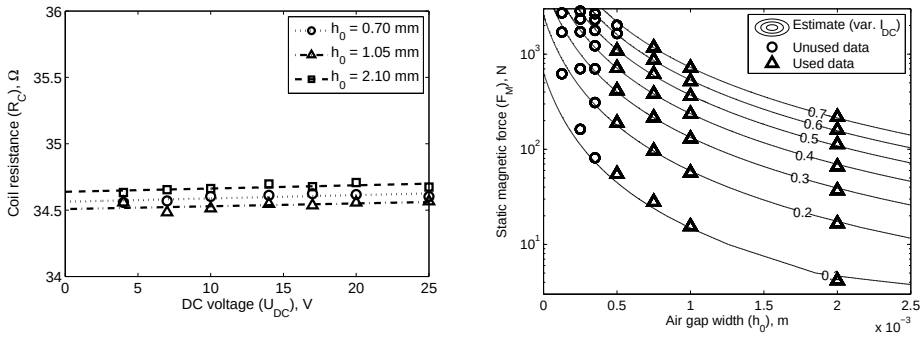

(a) (b)

Figur 6.2: (a) Resistance of electromagnetic coil as a function of DC voltage; (b) electromagnetic force as a function of air gap and comparison of the measurements and model (an estimate) (Darula et al., 2012)

6.2.1 Electromagnetic coil resistance

The resistance of the coil is characterized indirectly from the current and the voltage measurements at various DC voltage and air gap levels, as shown in Fig. 6.2a. As concluded in paper E (Darula et al., 2012), as the variation of the resistance is small, the value of R_C can be treated independent of air gap and current value and just the average value ($R_C = 34.6\Omega$) can be considered.

6.2.2 Static electromagnet force

To verify the model of the electro-magnetic force derived in Sec. 3.2.3, a static magnetic force is measured, where the triangular set-up with no passive stiffness elements was used. The parameters of the electromagnet, taken as initial estimates, are summarized in Appendix B.1.

The expression of electromagnetic force, Eq. (A.43), is modified to accommodate the measurements and as summarized in paper E (Darula et al., 2012), the estimate of the magnetic force is searched in the form:

$$F_{est} = \frac{C_e i_{DC}^2}{(l_0 + 2h)^2} \tag{6.1}$$

where C_e and l_0 are unknown parameters to be searched. The estimated and identified parameters are summarized in Table 3 of the paper E. A comparison of the measured forces and an estimate is shown in Fig. 6.2b.

6.2.3 Identification of the static deflection and limiting current

A theoretical analysis on static deflection and limiting current is summarized in (Stein et al., 2011) and a brief discussion was introduced in Sec. 4.1.

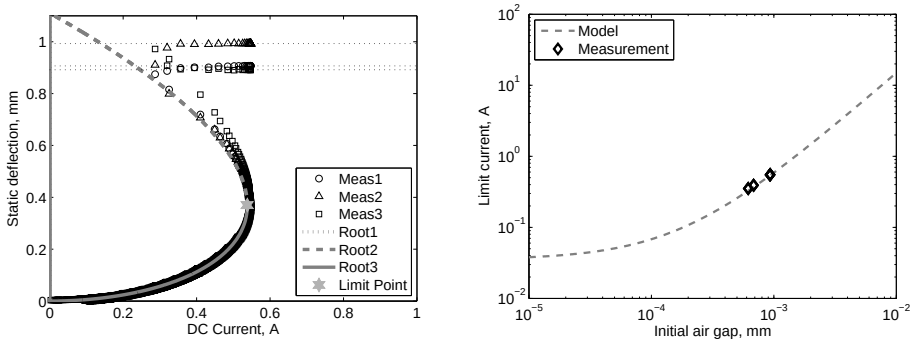

(a) (b)

Figur 6.3: (a) comparison of the analytical model (solving Eq. (4.1)) and measurements of static deflection of triangular set-up; (b) comparison of the model (Eq. (4.2)) and measurements of the limit current

A comparison of the model (using parameters estimated in the previous section) with measurements is presented in Fig. 6.3a. It can be seen, that in statics, the model correctly predicts the response of the system. Even the unstable root (above limit point) was recorded during measurements and it agrees with the model.

The estimation of the limiting current, i.e. maximal current which can be applied, is derived in Sec. 4.1 (Eq. (4.2)). Using the triangular set-up with passive springs installed (Fig. 6.1) and measuring simultaneously the current and displacement, the expression can be verified. As shown in Fig. 6.3b, the measurements were done for three levels of air gap. Since the triangular set-up was equipped with just one set of stiffness elements, only a single limiting current curve is presented in the figure.

6.3 Investigation of losses

An in-depth analysis of losses in the electromagnet used for experiments (Magnet-Schultz G MH) is summarized in paper E (Darula et al., 2012). In order to ensure a constant air gap, for the investigations presented in the paper, a triangular set-up was used with the armature firmly fixed.

As discussed in the paper, the equivalent loss resistance R_e is a function of an excitation frequency f and depends on the air gap width (h_0) as well as supply current (i_{DC}, paper E (Darula et al., 2012)):

$$R_e = \frac{R_{eE}\rho_{eH}f}{R_{eE} + \rho_{eH}f} \tag{6.2}$$

with parameters R_{eE} and ρ_{eH} used to describe the eddy current and hysteresis losses, respectively.

The parameters, describing eddy current and hysteresis losses, are identified from experimental data using a least square method (Ljung, 1999) and the chosen results are presented in Fig. 6.4. More in-depth discussion on results is summarized in the paper E (Darula et al., 2012).

6.4 Magnetization curve

The model presented in the paper E (Darula et al., 2012) used a concept of hysteresis losses. However the model implemented an equivalent resistance, so it did not directly separate the hysteresis and eddy current losses.

In order to investigate, if the hysteresis phenomenon is present in the electromagnet used for experiments, a simple magnetization curve measurements were performed. The electromagnet with a fixed air gap was exposed to AC current of different frequencies (as well as an quasi static case) and current amplitudes. As can be seen from Fig. 6.5, for large current values the magnetic material saturation can be reached and the hysteresis effect is also observable. At this stage of the project, no further analysis of the hysteresis phenomena has been done.

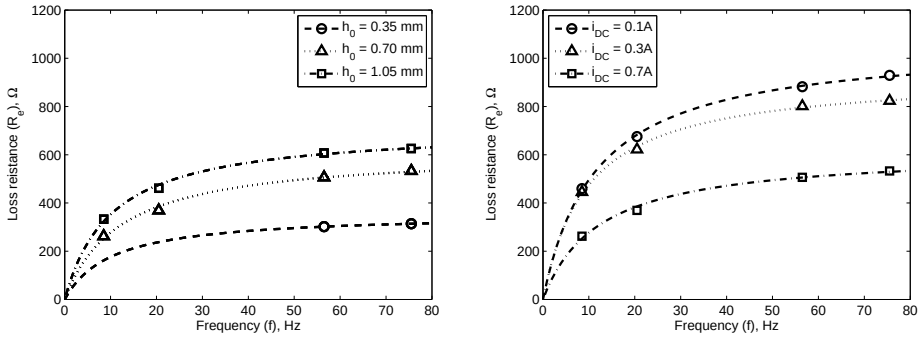

(a) (b)

Figur 6.4: Equiavalent loss resistance as a function of frequency and (a) variable air gap width (with current fixed at 0.7A); (b) variable current (and air gap fixed at 0.7 mm) (Darula et al., 2012)

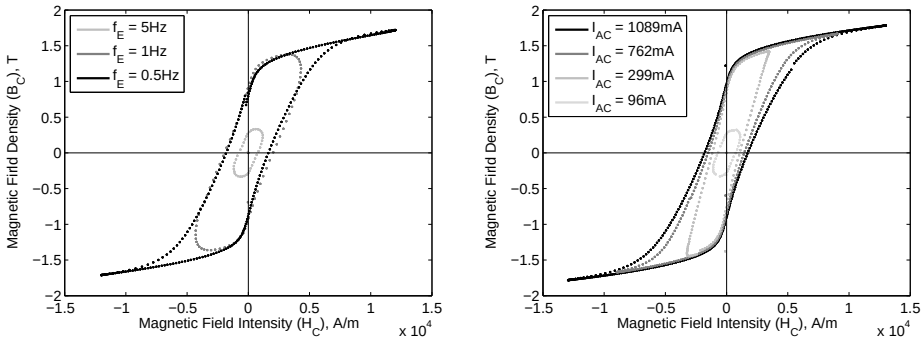

(a) (b)

Figur 6.5: B-H curve for (a) variable excitation frequency; (b) for quasi-static excitation frequency (0.5Hz) and variable AC current

6.5 Controller's operation

The experiments presented in this chapter proved, that for the electromagnet used (Magnet-Schultz G MH), the electromagnetic force is inversely proportional to the displacement, i.e. the concept of negative stiffness can be applied. Also the concept of limiting current was verified, so knowing the value of passive stiffness, an operation parameters (air gap width and supply current value) of the electromagnetic element can be chosen.

Furthermore the hysteresis as well as eddy current losses were identified and modelled using an equivalent loss resistance. Thus both concepts, namely natural frequency detuning and damping due to electromagnetic interaction, has been proved using isolated experiments.

In order to see if the controller is capable to combine both concepts, a beam

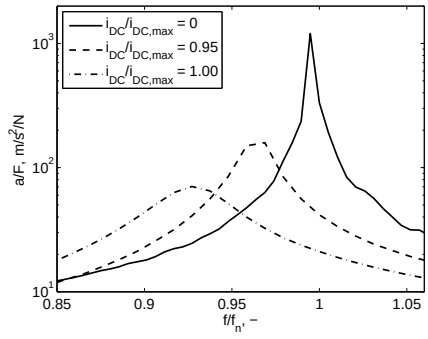

Figur 6.6: Frequency response functions of beam vibration with a controller

set-up was used (Fig. 6.1b). Vibration was excited using an impact hammer.

Due to the practical limits of electrical resistance, the operation region with maximal detuning has not been measured yet. As can be seen from Fig. 6.6, just the operation region 'detuning and damping' was reached at this stage of the project.

The dependency of the detuning as well as damping on electric current is presented in Fig. 6.7, where the values of natural frequency as well as damping were extracted directly from measured frequency response functions using a half-power bandwidth method (built-in function in Bruel&Kjaer PULSE LabShop software).

Results from both set-ups and different settings (weight/stiffness) are summarized in the figures. It can be seen that the detuning is a function of current (Fig. 6.7a), whereas the damping is effective only at high current values, i.e. for

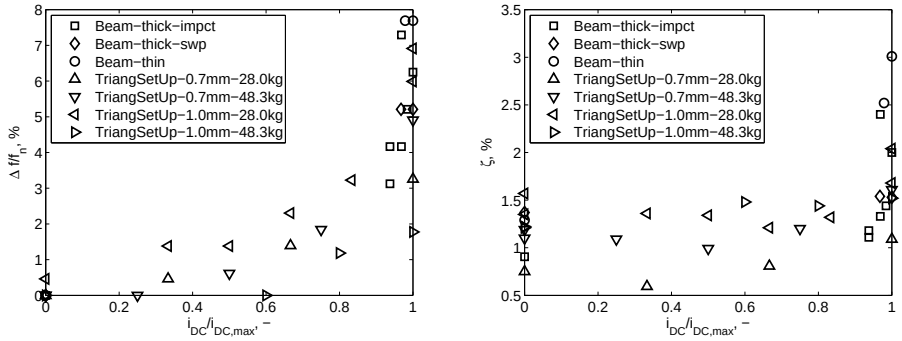

(a) (b)

Figur 6.7: (a) non-dimensional detuning and (b) relative damping as functions of non-dimensional current. Data extracted from measurements performed on both set-ups (beam as well as triangular plate) and for various air gap ($h_0 = 0.7$ and 1.0mm), weight of a dummy mass ($m_m = 28.0$ and 48.3kg) and stiffness values(thick/thin beam). At thick beam impact hammer and sine sweep (SWP) measurements with electrodynamic shaker were done, thin beam was measured using the impact hammer and triangular set-up with random noise shaker excitation.

relatively strong magnetic fields (Fig. 6.7b).

For the settings used in the experiments, the maximal detuning 8% and relative damping 3% was obtained (Fig. 6.7). From the theoretical analysis, the detuning up to 35% and damping 30% is theoretically possible to be obtained (Darula and Sorokin, 2012).

7 Discussion and conclusions

The thesis summarizes the three-years work on investigation of utilization of the electromagnetic elements in vibration control of heavy machinery.

Besides the five articles attached to the theses, seven additional papers were published to report the progress in the project and the results obtained.

The analytical model was used to characterize the operational regimes of the controller as well as to study a possible non-linear behaviour. The parameters for the model were identified experimentally.

Three operational regimes were identified, namely no action of the controller, natural frequency detuning with additional damping and pure natural frequency detuning.

The non-linear problem was solved analytically by means of a method of multiple scales and the solution was verified numerically. The study of the non-linear behaviour included also a stability analysis as well as possible modal interaction phenomena. The dangerous non-linear operation regimes were identified in order to avoid the undesirable non-linear effects in practical applications.

The vibration control strategy was analysed numerically (using MATLAB Simscape) and the feasibility of the controller's operation was verified by series of experiments. The results showed that both phenomena - natural frequency detuning and additional electro-magnetic damping - are feasible to be implemented in vibration control. For the set-up used 8% detuning and 3% damping were obtained.

7.1 Implementation of the electromagnetic elements

As discussed in previous sections, the electromagnetic elements can be used in applications where the control of natural frequencies and/or of amount of damping is requested. Thanks to the ability to produce relatively large control forces (up to the range of kN) and their robustness, the electromagnetic elements are suitable to control vibration of machinery of broad size scale.

Operation of these elements in the regimes identified in Sec. 4.2 is suitable e.g. for:

- **Control of vibration during machine's run-up/run-down** - to reduce time the system passes through resonance (analysed in Sec. 4.4).

- **Variable operation conditions of machinery** - where natural frequency can be changed and/or damping can be added to the system, when machinery changes its operation regime (e.g. varying the operation speed and/or increasing the excitation force/vibration due to imbalance, misalignment, etc.).

7.2 Contribution of the PhD work

The contribution of PhD work can be summarized as:

- A detailed non-linear analysis of electro-magneto-mechanical (1+1/2)DOF and (2+2x1/2)DOF systems.
- Analysis of modal interaction in a (2+2x1/2)DOF system.
- Parametric study on electromagnetic element's dynamical response.
- Determination of operation regimes and investigations of their stability.
- Experimental characterization of the system and proving detuning/damping concepts.
- Creating a demo set-up to prove the control strategy.

7.3 Future work

During the period PhD project was running, not all objectives listed in Sec. 1.2 were resolved equally thoroughly and some of the areas deserve more investigation:

- Creating more advanced model of the losses in the electro-magnetic circuits.
- Reducing the losses in the electro-magnetic system to increase the level of detuning.
- Experimental validation of the non-linear regimes.
- Parametric studies of a performance of the controller.
- Improvement of a control strategy - not working only as a switched device but add also some feed-back/feed-forward loop.
- Solving some stability issues of the real-life controller's application.

References

Andronov, A., A. Vitt, and S. Khaikin (1959). *Vibration theory*. Moscow, RUS: Fizmatgiz.

Behrens, S., A. Fleming, and S. Reza Moheimani (2003). Electromagnetic shunt damping. *Advanced Intelligent Mechatronics, 2003. AIM 2003. Proceedings. 2003 IEEE/ASME International Conference on 2*, 1145 – 1150.

Bishop, R. (2002). *The Mechatronics Handbook*. Boca Raton, USA: CRC Press.

Bonfitto, A., X. De Lepine, M. Silvagni, and A. Tonoli (2009). Self-sensing active magnetic dampers for vibration control. *Journal of Dynamic Systems, Measurement and Control, Transactions of the ASME 131*(6), 1–7.

Brennan, M. (2006). Some recent developments in adaptive tuned vibration absorbers/neutralisers. *Shock and Vibration 13*(4-5), 531–543.

Casciati, F., G. Magonette, and F. Marazzi (2006). *Technology of Semiactive Devices and Applications in Vibration Mitigation*. Chichester, UK: John Wiley & Sons.

Chakraborty, S. and G. Tomlinson (2003). Novel non-contact passive damping of structures: An experimental investigation using electromagnetic concepts. *Proceedings of the Institution of Mechanical Engineers, Part C: Journal of Mechanical Engineering Science 217*(9), 991–1000.

Cheng, D. (1989). *Field and Wave Electromagnetics* (2 ed.). Reading, USA: Addison-Wesley.

Chiba, A., T. Fukao, O. Ichikawa, M. Oshima, M. Takemoto, and D. Dorrell (2005). *Magnetic Bearings and Bearingless Drives*. Oxford, UK: Elsevier Science.

Daley, S., J. Hätönen, and D. Owens (2006). Active vibration isolation in a "smart spring"mount using a repetitive control approach. *Control Engineering Practice 14*(9), 991–997.

Darula, R. and S. Sorokin (2012). On non-linear dynamics of a coupled electromechanical system. *Nonlinear Dynamics 70*(2), 979–998.

Darula, R. and S. Sorokin (2013). An Analytical Study of Non-Linear Behaviour of Coupled 2+2x0.5 DOF Electro-Magneto-Mechanical System by the Method of Multiple Scales. In Rustighi, E., et al. (Ed.), *11th International Conference Recent Advances in Structural Dynamics (RASD 2013), July 1-3. Pisa, IT*, pp. 841.1–841.12.

Darula, R. and S. Sorokin (2014). Analysis of Multi-Physics Interaction Effects in a Coupled Dynamical Electro-Magneto-Mechanical (2+2x1/2)DOF system. *Journal of Sound and Vibration 333*(14), 3266–3285.

Darula, R., G. Stein, and S. Sorokin (2013). Numerical simulations of electromagnet exposed to vibration. *Engineering Mechanics 20*(6), 439–448.

Darula, R., G. J. Stein, C. S. Kallesøe, and S. Sorokin (2012). Mathematical modelling and parameter identification of an electro-magneto-mechanical actuator for vibration control. In Bernard, A., et al. (Ed.), *Proceedings of ASME 2012 11th Biennial Conference on Engineering Systems Design and Analysis*, Volume 2, pp. 291–300. American Society of Mechanical Engineers.

Darula, R., G. J. Stein, and S. Sorokin (2011). An application of electromagnetic induction in vibration control. In Naprstek, J., et al. (Ed.), *Vibration Problems ICOVP 2011*, Volume 139 of *Springer Proceedings in Physics*, pp. 447–453. Springer Netherlands.

de Silva, C. W. (2007). *Vibration Damping, Control, and Design* (1 ed.). Boca Raton, USA: CRC Press.

Dohnal, F. (2007). Suppressing self-excited vibrations by synchronous and time-periodic stiffness and damping variation. *Journal of Sound and Vibration 306*(1-2), 136–152.

Dohnal, F. (2012). Experimental studies on damping by parametric excitation using electromagnets. *Proceedings of the Institution of Mechanical Engineers, Part C: Journal of Mechanical Engineering Science 226*(8), 2015–2027.

Fitzgerald, A., C. Kingsley, and S. Umans (2003). *Electric Machinery* (6 ed.). New York, USA: McGraw-Hill.

Franchek, M., M. Ryan, and R. Bernhard (1996). Adaptive passive vibration control. *Journal of Sound and Vibration 189*(5), 565 – 585.

Fuller, C. C., S. J. Elliott, and P. A. Nelson (1997). *Active Control of Vibration*. London, UK: Academic Press.

Furlani, E. P. (2001). *Permanent Magnet and Electromechanical Devices. Materials, Analysis and Applications*. San Diego, USA: Academic Press.

Gospodarc, B., D. Voncina, and B. Bucar (2007). Active electromagnetic damping of laterally vibrating ferromagnetic cantilever beam. *Mechatronics 17*(6), 291 – 298.

Hinch, E. (1991). *Perturbation methods*. Cambridge texts in applied mathematics. Cambridge, UK: Cambridge University Press.

Hoque, M., T. Mizuno, Y. Ishino, and M. Takasaki (2012). A modified zero-power control and its application to vibration isolation system. *JVC/Journal of Vibration and Control 18*(12), 1788–1797.

Inman, D. (2006). *Vibration with Control*. Chichester, UK: John Wiley & Sons.

Kari, L. and P. Blom (2005). Magneto-sensitive rubber in a noise reduction context - exploring the potential. *Plastics, Rubber and Composites 34*(8), 365–371.

Karnopp, D., M. Crosby, and R. Harwood (1974). Vibration control using semi-active force generators. *Journal of Engineering for Industry, Transactions of the ASME 96 Ser B*(2), 619–626.

Krause, P. and O. Wasynczuk (1989). *Electromechanical Motion Devices*. New York, USA: McGraw-Hill.

Li, Z., X. Wang, M. Behrooz, N. Maus, and F. Gordaninejad (2012, March). A tunable 'negative' stiffness system for vibration control. In *Society of Photo-Optical Instrumentation Engineers (SPIE) Conference Series*, Volume 8341 of *Society of Photo-Optical Instrumentation Engineers (SPIE) Conference Series*.

Ljung, L. (1999). *System Identification: Theory for the User*. Upper Saddle River, USA: Pearson Education.

magnetschultz.co.uk (2010). Magnet Schultz, D.C. Holding Magnet Type GMH GZZ. Data Sheet. `http://www.magnetschultz.co.uk/docs/Electromagnets/GMH%20GZZ.pdf`.

Mizuno, T., M. Takasaki, D. Kishita, and K. Hirakawa (2007). Vibration isolation system combining zero-power magnetic suspension with springs. *Control Engineering Practice 15*(2), 187–196.

Mohan, N., T. Undeland, and W. Robbins (1995). *Power electronics: converters, applications, and design* (2nd ed.). New York, USA: John Wiley & Sons.

Nayfeh, A. (1991). *Perturbation methods*. New York, USA: John Wiley & Sons.

Nayfeh, A. (2000). *Nonlinear Interactions: Analytical, Computational, and Experimental Methods*. New York, USA: John Wiley & Sons.

Nitsche, R. and L. Gaul (2002). Damping control in systems assembled by semi-active joints. In A. Preumont (Ed.), *Responsive Systems for Active Vibration Control*, Volume 85 of *NATO Science Series*, pp. 239–251. Dordrecht, NL: Springer Netherlands.

Niu, H., X. Zhang, S. Xie, and P. Wang (2009). A new electromagnetic shunt damping treatment and vibration control of beam structures. *Smart Materials and Structures 18*(4), 1–15.

Panovko, Y. and I. Gubaniva (1987). *Stability and Vibration of Elastic Systems* (4 ed.). Moscow, RUS: Nauka.

Paulitsch, C., P. Gardonio, and S. J. Elliott (2006). Active vibration control using an inertial actuator with internal damping. *Journal of the Acoustical Society of America 119*(4), 2131–2140.

Rao, S. (2004). *Mechanical vibrations* (4 ed.). Upper Saddle River, USA: Addison-Wesley.

Saeed, T. E., G. Nikolakopoulos, J.-E. Jonasson, and H. Hedlund (2013). A state-of-the-art review of structural control systems. *Journal of Vibration and Control* -(-), 1–19.

Schmidt, E., W. Paradeiser, F. Dohnal, and H. Ecker (2007). Design of an electromagnetic actuator for parametric stiffness excitation. *COMPEL - The International Journal for Computation and Mathematics in Electrical and Electronic Engineering 26*(3), 800–813.

Schwartz, M. M. (2002). *Encyclopedia of Smart Materials*. New York, USA: John Wiley & Sons.

Sodano, H. and D. Inman (2008). Modeling of a new active eddy current vibration control system. *Journal of Dynamic Systems, Measurement and Control, Transactions of the ASME 130*(2), 0210091–02100911.

Stein, G., R. Darula, and R. Chmurny (2011). The limits of the beam sag under influence of static magnetic and electric force. *Engineering Mechanics 18*(5/6), 323–329. Available on-line: `http://www.engineeringmechanics.cz/pdf/18_5_323.pdf`.

Thomsen, J. J. (2004). *Vibrations and Stability. Advanced Theory, Analysis, and Tools* (2 ed.). Berlin Heidelberg, DE: Springer-Verlag.

Tonoli, A., N. Amati, and M. Silvagni (2008). Transformer eddy current dampers for the vibration control. *Journal of Dynamic Systems, Measurement and Control, Transactions of the ASME 130*(3), 1–9.

A
Derivations' details

The appendix summarizes additional derivations of the concepts used in the thesis.

A.1 Detailed derivations of the governing equations

As discussed in Ch. 3, a lumped parameter (1+1/2)DOF system was used (Fig. A.1) to derive governing equations and then the concept was used for (2+2x1/2)DOF model. Let us take again a (1+1/2)DOF system and analyse the subsystems more deeply.

A.1.1 Magnetic circuit

The Ampere's law defines a relationship between the magnetic field intensity (H) integrated about the closed path (L) to a net current ($i_m(t)$)(Cheng, 1989; Krause and Wasynczuk, 1989):

$$\oint \vec{H} d\vec{L} = N_w \vec{i_m}(t) \tag{A.1}$$

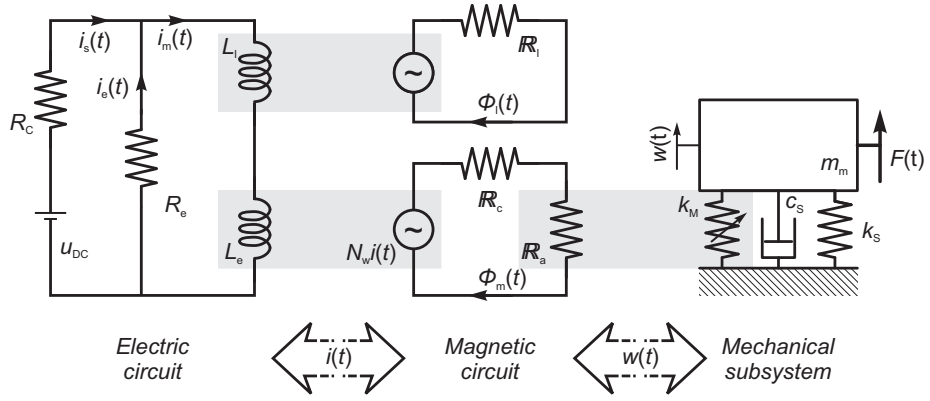

Figur A.1: Sketch of the sub-models with an indication of the coupling terms

where N_w is a number of turns of a coil.

As explained in Sec. 2.4, the magnetic flux in electro-mechanical systems, used for vibration control, enters two media - an iron core (a ferromagnetic material, described in equivalent model as a core reluctance $\Re_C$, Fig. A.1) and an air gap (described as an air reluctance $\Re_a$). Since the field intensity is a function of material, we need to re-write the Eq. (A.1):

$$\int H_C dL + \int H_g dL = N_w i_m(t) \qquad \Rightarrow \qquad H_C l_C + 2H_g h(t) = N_w i_m(t) \tag{A.2}$$

where H_C is a magnetic field intensity in the iron core and H_g the intensity in the air gap. The length l_C and $h(t)$ represent the equivalent flux length in the core and air gap, respectively. It needs to be noted, that as the flux path enters the air gap twice (Fig. 3.1), the equivalent length of the flux path in the air is $l_g = 2h(t)$.

If no fringing effects are assumed (it is valid for sufficiently small air gap, as used throughout the project), then the cross-sectional area of the flux path is constant ($S_C = S_g$). It also means that the magnetic flux density in the iron core as well as in the air gap are the same, i.e. $B_g(t) = B_C(t) = B(t)$. Noting that the magnetic flux is defined as $\Phi_m(t) = B(t)S_C$, it can be expressed as:

$$\begin{aligned} N_w i_m(t) =& H_C l_C + 2H_g h(t) = \frac{B_C l_C}{\mu_0 \mu_{rC}} + \frac{2B_g h(t)}{\mu_0} = \frac{B(t) l_C}{\mu_0 \mu_{rC}} + \frac{2B(t) h(t)}{\mu_0} \\ =& \frac{\Phi_m(t) l_C}{\mu_0 \mu_{rC} S_C} + \frac{2\Phi_m(t) h(t)}{\mu_0 S_C} \\ \Phi_m(t) =& \frac{N_w i_m(t)}{\frac{l_C}{\mu_0 \mu_{rC} S_C} + \frac{2h(t)}{\mu_0 S_C}} = \frac{\mu_0 S_C N_w i_m(t)}{\frac{l_C}{\mu_{rC}} + 2h(t)} \end{aligned} \tag{A.3}$$

One of sources of losses (discussed in Sec. 2.4.4) to be included in a model is a leakage flux (Φ_l). As expressed in (Krause and Wasynczuk, 1989):

$$\Phi_l = \frac{N_w i_m(t)}{\Re_l} = l_l i_m(t) \tag{A.4}$$

where $\Re_l$ is the leakage reluctance and l_l equivalent length of leakage flux path, which needs to be determined experimentally.

The total magnetic flux in the system is then expressed as a sum of magnetizing (Φ_m) and leakage flux (Φ_l):

$$\Phi(t) = \Phi_m(t) + \Phi_l(t) = \frac{\mu_0 S_C N_w i_m(t)}{\frac{l_C}{\mu_{rC}} + 2h(t)} + l_l i_m(t) \tag{A.5}$$

A.1.2 Electric circuit

Analysing a coil exposed into a variable magnetic field, the voltage ($u_i(t)$) induced in the coil as a result of the magnetic flux variation can be expressed using

Faraday's Law (Cheng, 1989):

$$u_i(t) = -N_w \frac{d\Phi}{dt} \tag{A.6}$$

$$u_i(t) = -N_w \frac{d}{dt}\left(\Phi_m + \Phi_l\right) = -N_w \frac{d}{dt}\left(\frac{\mu_0 S_C N_w i_m(t)}{\frac{l_C}{\mu_{rC}} + 2h(t)} + l_l i_m(t)\right) \tag{A.7}$$

As discussed in Sec. 2.4.4, the loss resistance R_e is used to model electrical losses and is added in parallel to the inductance (Fig. A.1). Then the magnetic (L_e) as well as leakage inductance (L_l) are functions of magnetic current i_m and the current dissipated at the loss resistance is denoted as i_e. According to Fig. A.1 $i_s = i_m - i_e$.

The Kirchhoff's circuit laws are applied to find the relationships between the currents and voltage:

$$u_{DC} = R_C i_s(t) - u_i(t) \tag{A.8}$$

$$u_{DC} - R_C i_s(t) = -R_e i_e(t) \tag{A.9}$$

where Eq. (A.7) can be substituted into Eq. (A.8):

$$u_{DC} = R_C i_s(t) + N_w \frac{d}{dt}\left(\frac{\mu_0 S_C N_w i_m(t)}{\frac{l_C}{\mu_{rC}} + 2h(t)} + l_l i_m(t)\right) \tag{A.10}$$

$$u_{DC} = R_C i_s(t) + L_l \frac{di_m(t)}{dt} + \frac{\partial \lambda(h(t), i_m(t))}{\partial t} \tag{A.11}$$

with a leakage inductance defined as $L_l = N_w l_l = N_w^2/\Re_l$ and the magnetic flux linkage as:

$$\lambda(h(t), i_m(t)) = N_w \Phi_m = \frac{\mu_0 A N_w^2 i_m(t)}{\frac{l_C}{\mu_{rC}} + 2h(t)} \tag{A.12}$$

$$\lambda(w(t), i_m(t)) = \frac{2C_e i_m(t)}{C_0 + w(t)} \tag{A.13}$$

$$h(t) = h_0 - h_{st} + w(t) \qquad C_e = \frac{\mu_0 S_C N_w^2}{4} \qquad C_0 = \frac{l_C}{2\mu_{rC}} + h_0 - h_{st} \tag{A.14}$$

Assuming linear material properties (i.e. operation on a linear region of a B-H curve):

$$\frac{\partial \lambda(w(t), i_m(t))}{\partial t} = -\frac{2C_e i_m(t)}{\left(C_0 + w(t)\right)^2}\frac{dw(t)}{dt} + \frac{2C_e}{\left(C_0 + w(t)\right)}\frac{di_m(t)}{dt} \tag{A.15}$$

Then using also Eq. (A.9)

$$\begin{aligned}\frac{R_e}{R_C+R_e}u_{DC} =& \frac{R_e}{R_C+R_e}R_C i_m(t) + \left(L_l + \frac{2C_e}{(C_0+w(t))}\right)\frac{di_m(t)}{dt} \\ &- \frac{2C_e i_m(t)}{(C_0+w(t))^2}\frac{dw(t)}{dt}\end{aligned} \tag{A.16}$$

The loss resistance and leakage inductance is introduced for experimental characterization analysed in paper E (Darula et al., 2012). For the remaining work $L_l = 0$ and $R_e \to \infty$ is considered, so:

$$u_{DC} = R_C i_m(t) + \frac{2C_e}{(C_0+w(t))}\frac{di_m(t)}{dt} - \frac{2C_e i_m(t)}{(C_0+w(t))^2}\frac{dw(t)}{dt} \tag{A.17}$$

A.1.3 Electro-magnetic force

The energy approach is used to determine the expression of the electromagnetic force. Following (Krause and Wasynczuk, 1989), force or torque of any electromechanical system found from:

$$dW_f = dW_e + dW_m \tag{A.18}$$

where W_f is energy stored in the coupling field, W_e is energy transferred to the coupling field by the electric system and W_m is the energy transferred by mechanical system.

Focusing on mechanical system and assuming the SDOF model, the equation of motion is:

$$m_m\frac{d^2w(t)}{dt^2} + c_S\frac{dw(t)}{dt} + k_S(-h_{st}+w(t)) = F(t) - F_m(t) \tag{A.19}$$

and the energy from mechanical system can be expressed as (Krause and Wasynczuk, 1989):

$$W_M = \int F(t)dw \tag{A.20}$$

$$\begin{aligned}W_M =& m_m\int\frac{d^2w(t)}{dt^2}dw + c_S\int\frac{dw(t)}{dt}dw \\ &+ k_S\int(-h_{st}+w(t))dw + \int F_m(t)dw\end{aligned} \tag{A.21}$$

with the first and the third terms being kinetic and potential energies of the system and the second term representing heat loss due to friction.

The total energy transferred to the coupling field from the mechanical system is

$$W_m = \int F_m(t)dw \tag{A.22}$$

The electric energy is determined from Eq. (A.11) (Krause and Wasynczuk, 1989):

$$W_E = \int u_{DC} i_m(t) dt \tag{A.23}$$

$$W_E = R_C \int i_m^2(t) dt + \int i_m(t) \frac{d\lambda(w(t), i_m(t))}{dt} dt \tag{A.24}$$

where the first term on the right hand side represents energy loss due to resistance and the last represents total energy transferred to the coupling field from the electric system:

$$W_e = \int e_f(t) i_m(t) dt = \int i_m(t) \frac{d\lambda(w(t), i_m(t))}{dt} dt$$
$$\Rightarrow \quad \frac{dW_e}{dt} = i_m(t) e_f(t) = i_m(t) \frac{d\lambda(w(t), i_m(t))}{dt} \quad \Rightarrow \quad dW_e = i_m(t) d\lambda \tag{A.25}$$

with e_f a voltage drop due to coupling field.

Then using so-called energy approach, i.e. taking energy as a function of flux linkage and position (Krause and Wasynczuk, 1989), then

$$dW_f(w(t), \lambda(t)) = dW_e(\lambda(t)) + dW_m(w(t)) \tag{A.26}$$

$$dW_f(w(t), \lambda(t)) = i_m(t) d\lambda(t) + F_m(t) dw(t) \tag{A.27}$$

$$dW_f(w(t), \lambda(t)) = \frac{\partial W_f(w(t), \lambda(t))}{\partial w(t)} dw(t) + \frac{\partial W_f(w(t), \lambda(t))}{\partial \lambda(t)} d\lambda(t) \qquad \Rightarrow$$
$$\frac{\partial W_f(w(t), \lambda(t))}{\partial w(t)} dw(t) + \frac{\partial W_f(w(t), \lambda(t))}{\partial \lambda(t)} d\lambda(t) = i_m(t) d\lambda(t) + F_m(t) dw(t) \tag{A.28}$$

$$\left(i_m(t) - \frac{\partial W_f(w(t), \lambda(t))}{\partial \lambda(t)} \right) d\lambda(t) = \left(\frac{\partial W_f(w(t), \lambda(t))}{\partial w(t)} - F_m(t) \right) dw(t) \tag{A.29}$$

which expresses a coupling between field energy $W_f(w(t), \lambda(t))$ and force $F_m(t)$. In the further derivations an assumption of no hysteresis losses is done, i.e. the single B-H curve considered (no loop) and the energy is assumed to be stored in a conservative manner, i.e. all coupling losses are assumed to be neglected.

Following (Krause and Wasynczuk, 1989), we will 'mathematically fix' the position of mechanical system associated with the coupling field and then excite the electrical system with the displacement held fixed (path O-A in Fig. A.2), i.e during excitation $w(t) = 0$, so $W_m = 0$ and then

$$W_f(t) = W_e(t) = \int e_f(t) i_m(t) dt = \int \lambda(t) di_m(t) \qquad \text{with } dw(t) = 0 \tag{A.30}$$

where for singly excited (one electric source) electromagnetic system holds $e_f = d\lambda/dt$.

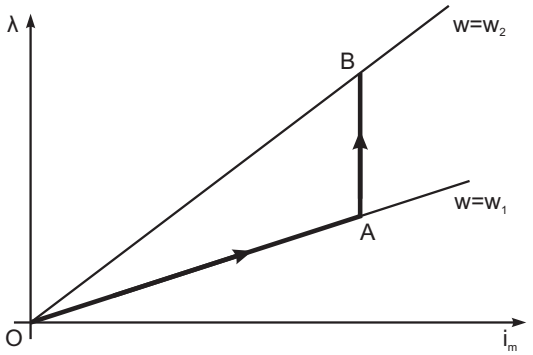

Figur A.2: Magnetic flux linkage (λ) as a function of magnetizing current i_m (Krause and Wasynczuk, 1989)

For magnetic flux linkage is valid

$$\begin{aligned} d\lambda(w(t), i_m(t)) &= \frac{\partial\lambda(w(t), i_m(t))}{\partial w(t)} dw(t) + \frac{\partial\lambda(w(t), i_m(t))}{\partial i_m(t)} di_m(t) \\ &= \frac{\partial\lambda(w(t), i_m(t))}{\partial i_m(t)} di_m(t) \qquad \text{with } dw(t) = 0 \end{aligned} \tag{A.31}$$

then the energy stored in the field of the singly excited system is

$$W_f(t) = \int \lambda(t) di_m(t) = \int i_m(t) \frac{\partial\lambda(w(t), i_m(t))}{\partial i_m(t)} di_m(t) \quad \text{with } dw(t) = 0 \tag{A.32}$$

The magnetic flux linkage is defined in Eq. (A.13) and its derivative reads:

$$d\lambda = \frac{2C_e}{(C_0 + w(t))} di_m(t) - \frac{2C_e i_m(t)}{(C_0 + w(t))^2} dw(t) \tag{A.33}$$

Using an energy approach ($dw(t) = 0$)

$$dW_f = dW_e = i_m d\lambda \qquad \text{with } dw(t) = 0 \tag{A.34}$$

where

$$d\lambda = \frac{2C_e}{(C_0 + w(t))} di_m(t) \qquad \text{with } dw(t) = 0 \tag{A.35}$$

$$W_f = \int_0^{i_m} i d\lambda = \int_0^{i_m} \frac{2C_e}{(C_0 + w(t))} i di = \frac{C_e i_m^2}{(C_0 + w(t))} \quad \text{with } dw(t) = 0 \tag{A.36}$$

Returning to original energy balance (Eq. (A.18)), i.e. $dW_f = dW_e + dW_m$, consi-

dering $w(t) \neq 0$:

$$dW_f = \frac{\partial W_f}{\partial i_m(t)} di_m(t) + \frac{\partial W_f}{\partial w(t)} dw(t) \tag{A.37}$$

$$dW_f = \frac{2C_e i_m(t)}{(C_0 + w(t))} di_m(t) - \frac{C_e i_m^2(t)}{(C_0 + w(t))^2} dw(t) \tag{A.38}$$

$$dW_e = i_m(t) d\lambda = \frac{2C_e i_m(t)}{(C_0 + w(t))} di_m(t) - \frac{2C_e i_m^2(t)}{(C_0 + w(t))^2} dw(t) \tag{A.39}$$

$$dW_m = F_m dw(t) \tag{A.40}$$

substituting it into $dW_f = dW_e + dW_m$ (Eq. (A.18))

$$\frac{2C_e i_m(t)}{(C_0 + w(t))} di_m(t) - \frac{C_e i_m^2(t)}{(C_0 + w(t))^2} dw(t) = ... \tag{A.41}$$

$$\begin{aligned} &\frac{2C_e i_m(t)}{(C_0 + w(t))} di_m(t) - \frac{2C_e i_m^2(t)}{(C_0 + w(t))^2} dw(t) + F_m(t) dw(t) \\ &- \frac{C_e i_m^2(t)}{(C_0 + w(t))^2} dw(t) = - \frac{2C_e i_m^2(t)}{(C_0 + w(t))^2} dw(t) + F_m(t) dw(t) \end{aligned} \tag{A.42}$$

$$F_m(t) = \frac{C_e i_m^2(t)}{(C_0 + w(t))^2} \tag{A.43}$$

which is valid for linear material properties, i.e. $\mu_{rC} = const.$

A.1.4 Mechanical system

The mechanical system represented by a simple SDOF mass-spring-damper system, which describes a motion of a mass m_m (characterized by an inertia force) on which the stiffness and damping forces are acting. The system is excited by an external force $F(t)$ and the electromagnetic element contributes with an force F_m.

Then using e.g, D'Alembert's principle, the equation motion becomes:

$$m_m \frac{d^2 w(t)}{dt^2} + c_S \frac{dw(t)}{dt} + k_S(-h_{st} + w(t)) = F(t) - F_m(t) \tag{A.44}$$

$$m_m \frac{d^2 w(t)}{dt^2} + c_S \frac{dw(t)}{dt} + k_S(-h_{st} + w(t)) + \frac{C_e i_m^2(t)}{(C_0 + w(t))^2} = F(t) \tag{A.45}$$

A.1.5 (2+2x1/2)DOF system

As discussed in Sec. 3.3, the (2+2x1/2)DOF system analysed in papers C and D (Darula and Sorokin, 2012, 2013) combines a 2DOF mechanical system with two electro-magnetic sub-systems (each with own electrical circuit), as sketched in Fig. A.3.

In order to describe the motion of mechanical system, generalized coordinates (a translation x_S and rotation θ_S) are used, whereas the electro-magnetic expressions

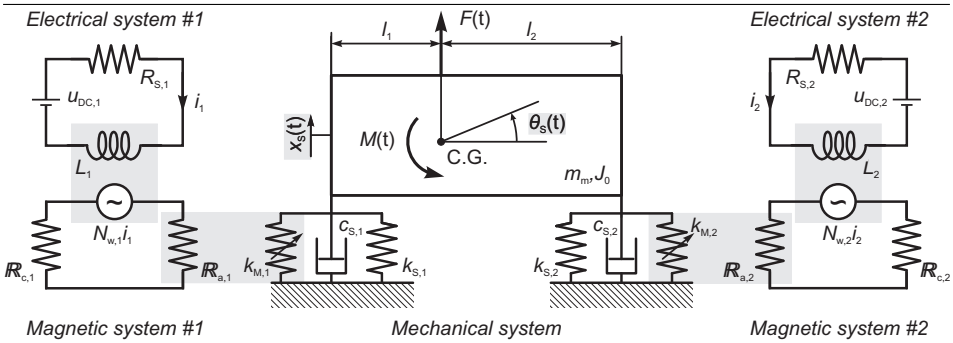

Figur A.3: Sketch of the (2+2x1/2)DOF electro-mechanical system (Darula and Sorokin, 2014)

are derived for displacement of each element (x_1, x_2), where $x_1 = x_S - l_1\theta_S$ and $x_2 = x_S + l_2\theta_S$.

The equations of motion are derived in paper D (Darula and Sorokin, 2014) applying a Lagrangian method. The kinetic energy considers the translational as well as rotational component:

$$T = \frac{1}{2} m_m \dot{x}_S^2 + \frac{1}{2} J_0 \dot{\theta}_S^2 \tag{A.46}$$

The passive stiffness elements contribute to potential energy:

$$V = \frac{1}{2} \sum_{n=1}^{2} k_n x_n^2 = \frac{1}{2} \sum_{n=1}^{2} k_n \left[x_S + (-1)^n l_n \theta_S \right]^2 \tag{A.47}$$

The electro-magnetic forces, as well as damping and external excitation forces are considered as generalized forces:

$$Q_x = F - \sum_{n=1}^{2} \left[c_S (\dot{x}_S + (-1)^n l_n \dot{\theta_S}) + F_{M,n} \right] \tag{A.48}$$

$$Q_\theta = M + \sum_{n=1}^{2} \left[c_n l_n (\dot{x}_S + (-1)^n l_n \dot{\theta_S}) - (-1)^n l_n F_{M,n} \right] \tag{A.49}$$

Then deriving the Lagrangian, the equations of motion are found in the form:

$$\begin{aligned} &m_m \frac{d^2 x_S}{dt^2} + (c_{S,1} + c_{S,2}) \frac{dx_S}{dt} + (-c_{S,1} l_1 + c_{S,2} l_2) \frac{d\theta_S}{dt} \ldots \\ &+ (k_{S,1} + k_{S,2}) x_S + (-k_{S,1} l_1 + k_{S,2} l_2) \theta_S + F_{m,1} + F_{m,2} = F \end{aligned} \tag{A.50}$$

$$\begin{aligned} &J_0 \frac{d^2 \theta_S}{dt^2} + (-c_{S,1} l_1 + c_{S,2} l_2) \frac{dx_S}{dt} + (c_{S,1} l_1^2 + c_{S,2} l_2^2) \frac{d\theta_S}{dt} \ldots \\ &+ (-k_{S,1} l_1 + k_{S,2} l_2) x_S + (k_{S,1} l_1^2 + k_{S,2} l_2^2) \theta_S - l_1 F_{m,1} + l_2 F_{m,2} = M \end{aligned} \tag{A.51}$$

The expression of electromagnetic force applied by each element is similar to Eq. (A.43), just the change of magnetic reluctance is described by the displacement at each element, i.e.

$$F_{m,n} = \frac{C_e(i_{DC,n} + i_{AC,n})^2}{(C_{0,n} + x_n)^2} = \frac{C_e(i_{DC,n} + i_{AC,n})^2}{(C_{0,n} + x_S + (-1)^n l_n \theta_S)^2} \tag{A.52}$$

Each electrical circuit is composed, similarly to circuit derived in Sec. 3.2.2, from resistance and inductance and the governing equation is similar to Eq. (A.16):

$$\begin{aligned} u_{DC,n} &= R_{S,n}(i_{DC,n} + i_{AC,n}) \ldots \\ &+ \sum_{m=0}^{3} \left[(-1)^m \frac{(1+m)C_e}{C_{0,n}} \frac{di_{AC,n}}{dt} (x_S + (-1)^n l_n \theta_S)^m \ldots \right. \\ &\left. - (-1)^m \frac{C_e(i_{DC,n} + i_{AC,n})}{C_{0,n}} (x_S + (-1)^n l_n \theta_S)^m \left(\frac{dx_S}{dt} + (-1)^n l_n \frac{d\theta_S}{dt} \right) \right] \end{aligned} \tag{A.53}$$

for the n-th circuit ($n = 1..2$).

B

Experimental set-ups and measurements

In the appendix information about experimental set-up and apparatus used is summarized.

B.1 Electromagnetic element

In the experimental part of the project an holding electromagnet Magnet-Schultz G MH×100×20 (magnetschultz.co.uk, 2010) was used. This industrial type of electromagnet was chosen as a device available on a market and capable to produce forces in the range of kN, which is of interest in applications of vibration control of heavy machines.

The geometrical and electrical parameters of the electromagnet used are summarized in Tab. B.1 and they are explained in Fig. B.1.

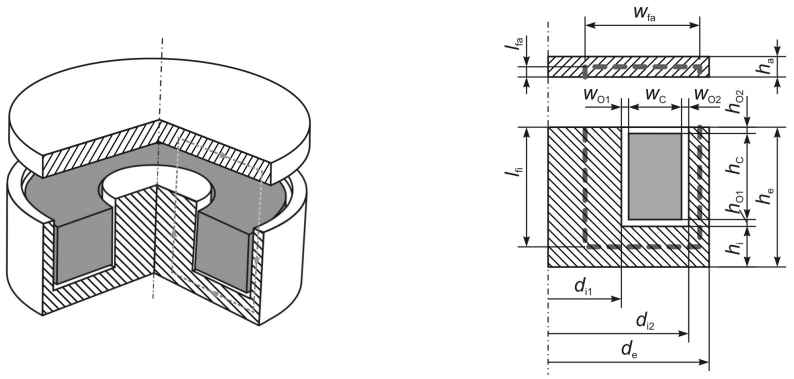

Figur B.1: Parameters of the electromagnet used in experimental verifications

Tabel B.1: Parameters of the electromagnet used in experimental verifications. Data from (magnetschultz.co.uk, 2010) and measured

Parameter	Value
Diameter of the electromagnet	$d_e = 100 \times 10^{-3}$m
Height of the electromagnet	$h_e = 43 \times 10^{-3}$m
Height of the armature	$h_a = 12 \times 10^{-3}$m
Inner diameter of the core	$d_{i1} = 47.5 \times 10^{-3}$m
Inner diameter of the rim	$d_{i2} = 87.8 \times 10^{-3}$m
Height of the core	$h_i = 12 \times 10^{-3}$m
Diameter of wire	$d_w = 0.5 \times 10^{-3}$m
Width of the core	$w_c = 16.75 \times 10^{-3}$m
Height of the core	$h_c = 27 \times 10^{-3}$m
Bottom off-set	$h_{01} = 1.5 \times 10^{-3}$m
Upper off-set	$h_{02} = 2.5 \times 10^{-3}$m
Inner off-set	$w_{01} = 1 \times 10^{-3}$m
Outer off-set	$w_{02} = 2.4 \times 10^{-3}$m
Core flux path height	$l_{fi} = 37 \times 10^{-3}$
Armature flux path height	$l_{fa} = 6 \times 10^{-3}$m
Flux path width	$w_{fa} = 35.075 \times 10^{-3}$m
Total flux path length	$l_f = 156.150 \times 10^{-3}$m
Core cross-sectional area	$S_C = 1.772 \times 10^{-3}$m^2
Power rating	$P_e = 17$W
Number of turns	$N_w = 1880$
Coil resistance	$R_C = 34.6\Omega$
Maximal force (zero stroke)	$F_m = 3700$N
Weight of armature	$m_a = 0.721$kg

Tabel B.2: Apparatus used

Device	Description
Magnet Schultz G MH$\times 100 \times 20$	Electromagnetic element (holding magnet)
Current measurement box (2pcs)	In-house
Voltage measurement box (2pcs)	In-house
Bruel&Kjaer PULSE 3506C	4ch dyn. and 4ch aux.(quasi static) data acq.box
Bruel&Kjaer 8202	Impact hammer
Bruel&Kjaer 4809	Electrodynamic shaker (10lbs)
Bruel&Kjaer 2706	Power amplifier
Techron 7540	Power amplifier
Bruel&Kjaer 4374	Miniature accelerometer
Bruel&Kjaer 2647A (4pcs)	Pre-amp. for accelerometer/impact hammer
Agilent E3649A	2ch DC power source
Bruel&Kjaer Vibro IN-081(2pcs)	Eddy current displacement transducer
Bently Nevada 21504	Eddy current transducer
Bently Nevada 7200 Proximitor	Amplifier for eddy current transducer
Mitutoyo 152-348	Micrometric screw used for eddy current calib.
HBM U9B (3pcs)	Force transducer (up to 5kN)
Synectic SY038I (3pcs)	Pre-amplifier for force transd.(current output)
Georg Reichter	Analog hardness test machine for force calib.

B.2 Apparatus used

The apparatus used for the measurements is listed in Tab. B.2. The heart of the apparatus is Bruel&Kjaer PULSE platform with B&K accelerometers and in-house volt and ammeters directly logged by B&K PULSE. The displacement was measured using eddy current transducers (B&K Vibro and Bently Nevada) and for calibration a micrometric screw (Mitutoyo) was used. Since also the static force was measured, strain-gauge based force transducers (HBM) were used instead of piezoelectric ones (which are capable to measure only dynamic forces). B&K PULSE used in experiments is capable to measure only voltage signal, therefore the pre-amplifiers were added as well. The electromagnet was powered by a DC power source (Agilent) and for hysteresis measurement the signal had to be amplified with a power amplifier (Techron). For excitation of vibration an electro-dynamic shaker B&K (with a B&K power amplifier) and B&K impact hammer was used.

B.2.1 Calibration of the displacement transducer

To measure the static (and dynamic) displacement, eddy current transducers were used (Bruel&Kjaer Vibro IN-081 and Bently Nevada 7200). The manufacturers do not provide a calibration sheet, since the sensitivity is dependent on sensing material.

In order to get the correct sensitivity level, a calibration rig, shown in Fig. B.2a was used. It consists of a transducer holder as well as a micro-metric screw (Mitutoyo 152-348) to determine the actual distance to be sensed.

The voltage values for some distances were logged, a calibration curves were plotted and the sensitivity as well as off-set was determined for a given sensing plates, used in actual set-up.

The calibration curves are shown in Fig. B.2b and the sensitivity and offset values are listed in Tab. B.3.

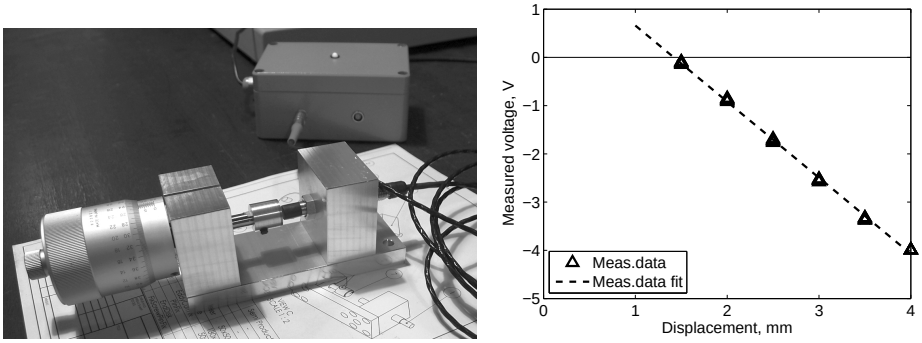

(a) (b)

Figur B.2: (a) eddy current transducer calibration set-up; (b) calibration curve

Tabel B.3: Calibration of the eddy current transducers

Notation	Transducer	Sensitivity [V/mm]	Offset [mm]
EddCr1	B&K IN-081	-1.730	1.2023
EddCr2	B&K IN-081	-1.723	1.2456
EddCr3	Bently Nevada 7200	-1.508	0.027

B.2.2 Calibration of force transducers

In order to be able to log dynamical as well as static forces a strain-gauge based force transducers HBM U9B were used. Since the data acquisition used (B&K PULSE 3506C) does not support directly strain gauge transducers, pre-amplifiers Synectic SY038I were used. The current version of the pre-amplifer was chosen in order to reduce the noise level. To measure the voltage signal (which can be processed by the data acquisition system) a set of resistors was used. Adding all the elements into a measurement chain, a calibration for each set of transducer-pre-amplifer was required.

The force transducers were calibrated statically using an analog hardness test machine Georg Reichter (Fig. B.3). The calibration curves are presented in Fig. B.4 and values listed in Tab. B.4.

Tabel B.4: Calibration of the force transducers

Notation	Serial no.	Sensitivity [mV/N]	Offset [N]
Frc1	111530145	1.2974	1010.554
Frc2	111530147	1.2433	1256.997
Frc3	111530146	1.1102	1311.926

(a) (b)

Figur B.3: (a) An overview on force transducer calibration set-up; (b) zoom to the transducer fixation in a machine

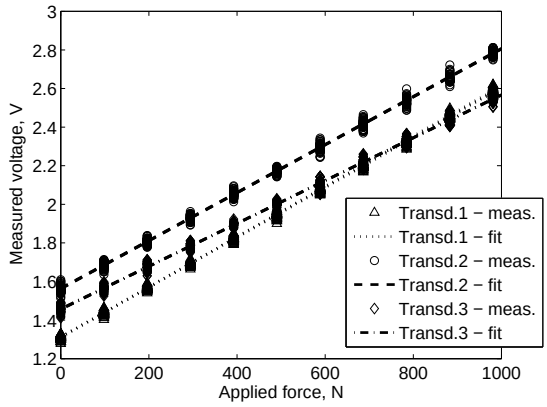

Figur B.4: Calibration curve for transducers

B.3 Experimental set-ups

As noted in Ch. 6, two set-ups were used in experimental characterization of the controller, namely a triangular and a beam.

B.3.1 Triangular set-up

The sketch of the triangular set-up with elements explained is presented in Fig. B.5.

This arrangement allowed us to measure the forces in the passive springs as well as displacements, so the adjustment of the air gap was more precise and from the measurements more information about the dynamics of the system was obtained.

Removing the passive springs, a static electromagnetic force was measured directly using three force transducers.

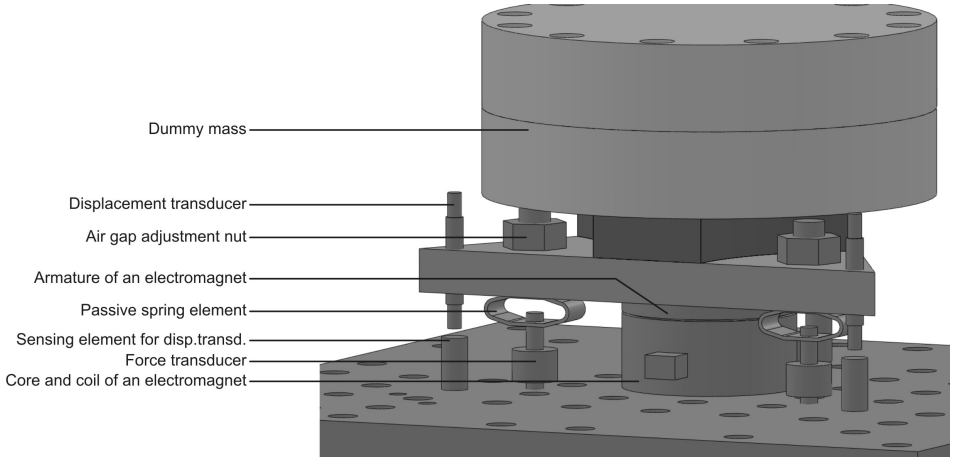

Figur B.5: Model of the triangular set-up

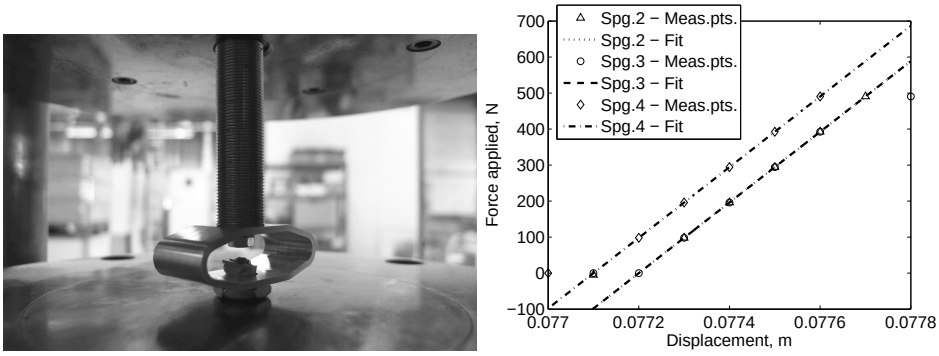

(a) (b)

Figur B.6: (a) A spring element under test; (b) calibration curves

Characterization of passive spring elements

The spring elements were designed to be compact, yet provide stiffness of $\mathcal{O}(10^6\text{N/m})$, so the trapezoidal shape was employed. A pre-evaluation of the stiffness was done analytically and using FEM interface in SolidWorks.

The stiffness was characterized indirectly, measuring the force and displacement using the same machine as for calibration of force transducers (a hardness testing machine Georg Reichter, Fig. B.6a). The stiffness element no.1 was damaged when too much force was applied, so just the elements no.2-4 were characterized and used later in measurements. Analysing the calibration curves (Fig. B.6b), the stiffness of each element is around $9.81 \times 10^5\text{N/m}$.

Since the actual stiffness depends also on the fixation of the spring elements to the set-up, the measured stiffness was taken as an initial estimate and the actual value of equivalent passive stiffness was evaluated from the natural frequency, knowing the moving mass.

B.3.2 Beam set-up

The beam set-up used in experiments is presented in Fig. B.7. Since the triangular set-up showed the feasibility to apply the electromagnetic elements for control vibration, the beam set-up was used also to reduce the amplitude of magnetic reluctance variation, as positioning the element closer to the clamped end, the displacement of the beam is smaller. The optimal location of the controller is left out for the further work.

The stiffness of the beam was assessed analytically and verified/tuned using a modal analysis.

All in all two beams of different stiffnesses and end masses were used, as summarized in Tab. B.5, listing corresponding natural frequencies. The controller was located in the same place for both beam set-ups.

Tabel B.5: Beams used in the experiment

Name	$f_{n,1}$
Thick-small mass	27Hz
Thin-small mass	13Hz

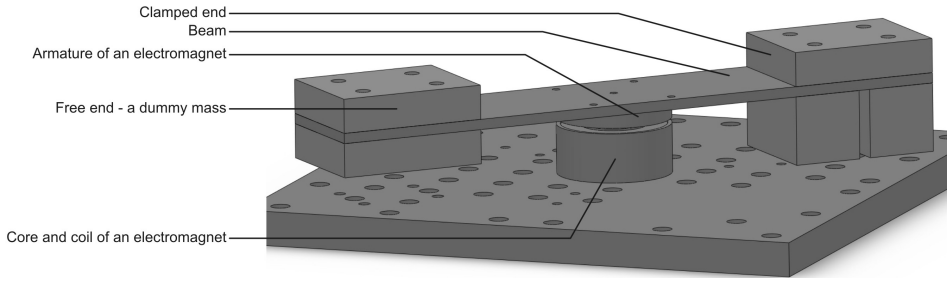

Figur B.7: Model of the beam set-up

Paper A

Paper Title: An Application of Electromagnetic Induction in Vibration Control
Authors: **Darula, R.**, Stein, G. J., Sorokin, S.
Published in: In Marvalova, B: Proceedings of the 10th biennial International Conference on Vibration Problems ICoVP 2011, Prague. Liberec, CZE: Technical university of Liberec, Springer Proceedings in Physics, Volume: 139, Pages: 447-453,
ISBN: 978-94-007-2068-8.
DOI: 10.1007/978-94-007-2069-5_61

Abstract

Excessive vibration of machines and/or structures can be controlled passively (e.g. introducing resilient elements) and/or actively (e.g. using elements capable to adjust their properties for actual state of the vibration).An electromagnet, as a vibration control element, can be implemented in active (or semi-active) control strategy. This approach is analyzed in the present paper. The electromagnetic induction occurs in a magnetic circuit exposed to variable magnetic flux, which can be obtained e.g. by changing reluctance (magnetic resistance) of the system due to a variable air gap, as the result of armature vibration. The lumped parameter mathematical model of the coupled electro-magneto-mechanical system is formulated. The performance of the model is analyzed, assuming harmonic forced vibration. By the induction, mechanical energy of vibration is converted into electrical one and dissipated in the shunt resistance. Two concepts are investigated further – electromagnet behaves as (a) a spring element (reduction of equivalent system stiffness); (b) a damping element.

Paper B

Paper Title: On non-linear dynamics of a coupled electro-mechanical system
Authors: **Darula, R.**, Sorokin, S.
Published in: *Nonlinear Dynamics*. Vol. 70, No 2, 2012, p. 979-998.
DOI: 10.1007/s11071-012-0505-0.

Abstract

Electro-mechanical devices are an example of coupled multi-disciplinary weakly non-linear systems. Dynamics of such systems is described in this paper by means of two mutually coupled differential equations. The first one, describing an electrical system, is of the first order and the second one, for mechanical system, is of the second order. The governing equations are coupled via linear and weakly non-linear terms. A classical perturbation method, a method of multiple scales, is used to find a steadystate response of the electro-mechanical system exposed to a harmonic close-resonance mechanical excitation. The results are verified using a numerical model created in MATLAB Simulink environment. Effect of non-linear terms on dynamical response of the coupled system is investigated; the backbone and envelope curves are analyzed. The two phenomena, which exist in the electro-mechanical system: (a) detuning (i.e. a natural frequency variation) and (b) damping (i.e. a decay in the amplitude of vibration), are analyzed further. An applicability range of the mathematical model is assessed.

Paper C

Paper Title: An Analytical Study of Non-Linear Behaviour of Coupled 2+2x0.5 DOF Electro-Magneto-Mechanical System by the Method of Multiple Scales

Authors: **Darula, R.**, Sorokin, S.

Published in: In Rustighi, E., et al.: RASD 2013, 11th International Conference Recent Advances in Structural Dynamics, July 1-3. Pisa, IT. p.841.1-841.12. ISBN 978-08-543-2964-9.

Abstract

An electro-magneto-mechanical system combines three physical domains - a mechanical structure, a magnetic field and an electric circuit. The interaction between these domains is analysed for a structure with two degrees of freedom (translational and rotational) and two electrical circuits. Each electrical circuit is described by a differential equation of the 1st order, which is considered to contribute to the coupled system by 0.5 DOF. The electrical and mechanical systems are coupled via a magnetic circuit, which is inherently non-linear, due to a non-linear nature of the electro-magnetic force. To study the non-linear behaviour of the coupled problem analytically, the classical multiple scale method is applied. The response at each mode in resonant as well as in sub-harmonic excitation conditions is analysed in the cases of internal resonance and internal parametric resonance.

Paper D

Paper Title: Analysis of Multi-Physics Interaction Effects in a Coupled Dynamical Electro-Magneto-Mechanical (2+2x1/2)DOF system
Authors: **Darula, R.**, Sorokin, S.
Published in: *Journal of Sound and Vibration*. Vol. 333, Issue 14, 2014, p. 3266-3285. DOI: 10.1016/j.jsv.2014.03.006.

Abstract

The operation of electro-magneto-mechanical systems involves the interaction of these three physical domains. In the paper, this interaction is analysed for a lumped parameter model, which consists of a two degrees of freedom (2DOF) linear mechanical system coupled via a nonlinear electro-magnetic field with two electrical circuits, contributing with 1/2DOF each. Dynamics of this multi-physical model is considered both in the nonlinear and in the linearised problem formulations. In the former case, the method of multiple scales is used to describe softening and modal interaction phenomena. The $2-1$ (super-harmonic) internal resonance is investigated, where stability and jump phenomena are analysed. The regimes of uni- and bi-modal responses are identified and a parametric study performed. The mathematical description of nonlinearities, introduced by multi-physical coupling, is compared with the classical formulation of nonlinear stiffness of a spring. For the linearised problem, the equivalent stiffness and the damping, as functions of the parameters of electro-magnetic elements, are assessed. The ranges of these parameters, when the nonlinear multi-physics interaction effects are suppressed by the dissipation effects of the same origin, are identified. The analytical predictions are verified by the numerical simulations. The relevance of the reported results to the operation of electro-magnetic adaptive passive control systems, capable to alter a natural frequency and add damping, is discussed.

Paper E

Paper Title: Mathematical Modelling and Parameter Identification of an Electro-Magneto-Mechanical Actuator for Vibration Control
Authors: **Darula, R.**, Stein, G.J., Kallesøe, C. S., Sorokin, S.
Published in: In Bernard, A. ASME 2012 11th Biennial Conference on Engineering Systems Design and Analysis (ESDA2012), Vol. 2, July 2-4, 2012. Nantes, FR: ASME, 2012. p. 291-300.
ISBN 978-0-7918-4485-4.
DOI:10.1115/ESDA2012-82167.

Abstract

An electro-magneto-mechanical system, composed of the electromagnet, having an iron core with a coil and a movable yoke, is analyzed in the paper. Exposing the yoke to mechanical motion, the variation of the magnetic flux due to change of the air gap height induces alternating voltage at the coil terminals. If the electrical circuit is closed, the so generated electrical power is dissipated via the internal coil losses, treated in this paper. Thanks to the interaction between the electrical and mechanical system (i.e. via magnetic force), the power dissipation in electrical circuit influences the dynamical response of the mechanical system. And so the mechanical vibrations can be controlled by these means.

The mathematical model of the simplified dynamical system, which describes behavior of the experimental set-up, is derived using a lumped parameter approach.

The aim of the article is to identify parameters of the derived mathematical model, focused mainly on electrical circuit. Based on measured experimental data, the static constants as well as dynamic losses were analyzed.